THE ASTROPHYSICAL JOURNAL, 414:580–600, 1993 September 10

THE α-ENHANCED ISOCHRONES AND THEIR IMPACT ON THE FITS TO THE GALACTIC GLOBULAR CLUSTER SYSTEM

MAURIZIO SALARIS,[1,2] ALESSANDRO CHIEFFI,[1] AND OSCAR STRANIERO[2]
Received 1992 August 12; accepted 1993 March 22

ABSTRACT

We analyze in detail the effect produced by the enhancement of the α-elements O, Ne, Mg, Si, S, and Ca on the evolutionary properties of low-mass, low-metallicity stars. In particular we address the evolutionary phases which extend from the main sequence up to the H reignition on the asymptotic giant branch. We find that the α-elements other than O cannot be neglected. Our main results are as follows:

1. Evolutionary models (suitable for Population II stars) with α-enhanced chemical composition can be computed even though proper low-temperature opacities are not yet available, since we demonstrate that most of the evolutionary properties of Population II stellar models (i.e., the location, in the H-R diagram, of both the main sequence and the turn off; the central H-burning lifetime; the luminosity of the bump on the red giant branch; the efficiency of the first dredge-up; the He core mass and the luminosity at the He flash; and the properties all along the following He-burning phase) are not influenced by the metal content included in the opacity coefficient below 12,000 K.

2. If the condition

$$\left[\frac{X_C + X_N + X_O + X_{Ne}}{X_{Mg} + X_{Si} + X_S + X_{Ca} + X_{Fe}}\right] \simeq 0$$

is satisfied once the α-elements have been enhanced (not necessarily by the same amount), then the α-enhanced isochrones are very well mimicked by the standard scaled solar isochrones of metallicity:

$$Z = Z_0(0.638 f_\alpha + 0.362)\,,$$

where f_α is the chosen average enhancement factor of the α-elements and Z_0 is the initial (nonenhanced) metallicity.

3. We discuss the fit to Groombridge 1830, the most "reliable" of the local subdwarfs, and we conclude that it is unnecessary, at present, to revise the value of the mixing-length parameter α [$\equiv l/H_p$] obtained by fitting the Sun.

4. The use of O-enhanced models is discouraged, since they lead to results which differ from those obtained by including the other α-elements.

5. We discuss the effect of the enhancement of the α-elements on the absolute and relative ages of the Galactic globular clusters by means of two independent methods, i.e., the ΔV(HB − TO) and the $\Delta(B-V)$ methods. Both lead to similar results: the absolute and the relative ages are only slightly affected by the enhancement of the α-elements. In particular, the ages obtained by adopting the $\Delta(B-V)$ method are practically insensitive to the enhancement, since this quantity depends only weakly on the metallicity, while the ones obtained by using the ΔV(HB−TO) method show a maximum decrease (by $\cong$0.7 Gyr per 0.3 dex in the overabundance) at the very low metallicity end ([M/H] $\cong -2.3$), which progressively reduces as the metallicity increases.

Subject headings: globular clusters: general — stars: abundances — stars: evolution — stars: interiors

1. INTRODUCTION

The study of the Galactic globular cluster (GGC) system has received long-standing attention owing to its importance in retaining precious information concerning the very first phase of the formation of our Galaxy. The high quality of the CCD data and the production of refined theoretical isochrones have led in these last few years to more quantitative comparisons between theory and observations than were possible prior to the 1980s.

With regard to the theoretical models, over the last decade essentially three sets of models devoted to the study of the GGCs became available: the first set, produced by Vanden-Berg & Bell (1985, hereafter VB85), extends from the lower main sequence (MS) up to the subgiant branch; the second, by Green, Demarque, & King (1987), and the third, by Chieffi & Straniero (1989, hereafter Paper I) and Straniero & Chieffi (1991, hereafter Paper II), both extend from the lower MS up to the red giant tip; we refer the reader to Papers I and II for a comparison among these three sets of models.

Most of the models produced up to now, including these three sets, were obtained by assuming scaled solar abundances for the elements heavier than He. However, in this last decade it has become progressively and definitely clear that the abundances of some elements, in particular the α-elements, are enhanced with respect to iron in Population II stars.

As far as we know, Simoda & Iben (1968, 1970) were the first to address the problem of the influence of the individual chemical species, other than helium and the average-metallicity "Z,"

[1] Istituto di Astrofisica Spaziale del CNR, CP 67, I-00044 Frascati, Italy.
[2] Osservatorio Astronomico di Collurania, I-64100 Teramo, Italy.

on the evolution of typical low-mass Population II stars. By comparing opacity tables for different metallicities (Cox & Stewart 1970a, b), they found that the elements beyond the He contribute to the opacity in only two well-defined regions, namely, at temperatures around 10^5–10^6 K and below 4×10^3 K. They analyzed only the region between 10^5 and 10^6 K, since none of their models reached an effective temperature lower than 5800 K. By computing appropriate opacity tables, they found that the continuum opacity around 10^5–10^6 K is mainly controlled by C, N, O, and Ne, and, since oxygen is the most abundant of this quartet, it is also the "biggest contributor." Concerning the behavior of the line opacity, they made no tests and *suggested* that, "on the average, C, N, and O are comparable in importance with metals as contributors" to the opacity. In addition, they showed that the turn off (TO) luminosity depends almost exclusively on the nuclear burning (i.e., on the global abundance of C, N, and O), while the effective temperature (i.e., the radius) is mainly controlled by the opacity. Since oxygen influences both the efficiency of the CNO burning and the opacity (at least the continuum opacity), it follows that, being also the most abundant of the elements beyond He, oxygen plays the key role in determining the evolutionary properties of a low-mass Population II star.

The same problem was addressed by Renzini (1977) a few years later. By analyzing the more recent opacity tables by Cox & Tabor (1976), he reached a conclusion rather similar to that obtained by Simoda & Iben (1968, 1970), i.e., that the elements heavier than He contribute to the opacity in only the two ranges of temperature already identified by Simoda & Iben. In addition, by speculating on the dependence of the opacity in these two regions on various chemical species, he suggested that the main "indirect" contributors to the opacity below 4×10^3 K are Mg, Si, and Fe because they are the ones with the lowest first-ionization potential and a nonnegligible abundance, while the dominant contributors in the region around 10^6 K are C, N, O, and Ne because their abundances "represent about 93% by number of the heavy elements." As a consequence of such speculation, he predicted that "the TO characteristics (stellar age, luminosity and effective temperature at the TO) depend primarily on Z_{CNO}," while the location of the RGB "depends primarily on the abundances of Fe, Si and Mg."

Renzini's predictions were checked a few years later by Rood (1981). He compared two evolutionary tracks of a typical Population II star, the first one computed by enhancing C, N, and O by a factor of 10 and the second one computed by enhancing all the heavy elements (except C, N, and O) by the same factor. He found that (*a*) in both cases the region extending from the MS up to the TO is shifted toward lower effective temperatures and luminosities (by a similar amount), (*b*) the slope of the red giant branch (RGB) depends only on the heavy elements other than C, N, and O, (*c*) the He core mass and the luminosity at the He flash depend only on the CNO abundance, and (*d*) the luminosity bump on the RGB depends on both.

Later, Bazzano et al. (1982) computed several evolutionary tracks from the MS up to the TO with enhanced CNO elements, and they confirmed Rood's result.

More recently VandenBerg and coworkers presented a series of models (and isochrones) (VandenBerg 1985; Fahlman, Richer, & VandenBerg 1985; Hesser et al. 1987; VandenBerg 1992; and Bergbusch & VandenBerg 1992) computed by enhancing the oxygen.

The influence of CNO on the evolutionary properties of horizontal-branch (HB) stellar models was first analyzed by Hartwick & VandenBerg (1973) and later by Castellani & Tornambè (1977), who found that an overabundance of CNO by a factor of 3 was enough to change and HB from blue to red.

Alongside these theoretical studies, a growing amount of data has accumulated in the last couple of decades, almost all showing that low-metallicity, low-mass stars are very probably enhanced in all of the α-elements, i.e., O, Ne, Mg, Si, S, and Ca (see, e.g., Lambert 1989).

This observational material can be roughly divided into three groups: data concerning field dwarfs, field giants, and globular cluster stars.

With regard to the field dwarfs, we refer to Sneden, Lambert, & Whitaker (1979), who find [O/Fe] = 0.5 in a dozen metal-poor stars; to Clegg, Lambert, & Tomkin (1981), who find a constant [O/Fe] = 0.6 and a constant [S/Fe] = 0.4 below [Fe/H] = 1; to Peterson (1981), who finds that Mg, Si, Ca, and Ti are overabundant by 0.2 dex with respect to the iron in 30 metal-poor field dwarfs and subgiants; to Magain (1985), who finds the α-elements overabundant by a factor of 0.4–0.6 in two metal-poor stars; to Barbuy, Spite, & Spite (1985), who find Ca overabundant in three metal-poor stars; to Tomkin, Lambert, & Balachandran (1985), who analyze 20 field stars, reaching the conclusion that [Mg/Fe] = [Si/Fe] = [Ca/Fe] = 0.4; to François (1986a, b), who finds Mg and Si to be overabundant by 0.4 in a sample of field metal-poor stars; to Laird (1986), who quotes [Mg/Fe] = 0.24 below [Fe/H] = −1.0, having analyzed 108 field dwarfs of various metallicities; to Magain (1987), who finds Mg, Si, and Ca to be overabundant by 0.4 dex in 20 field stars; and to Zhao & Magain (1990), who quote [Ca/Fe] = 0.48 in 20 stars.

With regard to the field giants, let us recall the papers by Leep & Wallerstein (1981), who find a large scatter in [O/Fe] (−0.1 to 0.8) but a clear overabundance of Ca by 0.6 dex in 11 stars; by Luck & Bond (1981), who find Mg and Si to be overabundant with respect to the Fe by ≈0.2–0.5 in 17 stars; by Luck & Bond (1985), who find a constant overabundance of O and Ca (∼0.5 dex), in a sample of 36 stars; by Gratton & Ortolani (1986), who quote [O/Fe] = 0.5 for a sample of 18 stars; by Gratton & Sneden (1987), who find [Mg/Fe] = 0.3, [Si/Fe] = 0.4, and [Ca/Fe] = 0.2 in a sample of 46 stars; by Barbuy (1988), who finds an overabundance of O by 0.35 dex in 20 stars; and by Magain (1989), who quotes an overabundance of Mg, Si, and Ca by ∼0.4 dex in a sample of 20 stars.

Let us remark at this point that, although all the papers cited above give quantitative estimates of the overabundances, which may differ by a few dex from one author to another, all of them show that the overabundance of each α-element tends to be almost constant below [Fe/H] ≈ −1.0. Contrary to such a common result Abia & Rebolo (1989) found an oxygen overabundance which increases monotonically as Fe decreases, reaching [O/Fe] = 1.0–1.2 at [Fe/H] = −2. Such a result has been refused by Bessell, Sutherland, & Ruan (1991) and by Spite & Spite (1991), who reanalyzed some of the metal-poor giants already studied by Abia & Rebolo by finding [O/Fe] = 0.5. We refer the reader to the quoted papers for a deep discussion of the problem.

Works devoted to the analysis of globular cluster stars include the works by Cohen (1978), who suggests that [O/Fe] ∼ 0.4 in M3 and M13 and that Mg, Si, and Ca are somewhat overabundant; by Pilachowski, Wallerstein, & Leep

(1980), who find that [O/Fe] ~ 0.4 in M3 and M5 and [O/Fe] ~ 0 in M13, while the α-elements Si and Ca tend to be overabundant ([Si/Fe] ~ 0.3); by Pilachowski, Sneden, & Wallerstein (1983), who suggest that the GGCs may be divided into two groups, the "normal" clusters having all the α-elements overabundant by ~ 0.3 dex and the "peculiar" clusters having [O/Fe] solar or even deficient; by Gratton, Quarta, & Ortolani (1986), who find that [α/Fe] ~ 0.27 in five clusters, i.e., 47 Tucanae, M4, M5, NGC 6752, and M71; by Gratton (1987), who finds Mg, Si, and Ca to be overabundant with respect to Fe (~ 0.3 dex) in five clusters, i.e., NGC 288, NGC 362, NGC 5897, NGC 6352, and NGC 6362; by Gratton & Ortolani (1989), who analyze the clusters NGC 1904, NGC 3201, NGC 4590, NGC 4833, NGC 6254, NGC 6397, and NGC 6656, finding that O, Mg, Si, and Ca are more or less equally overabundant by ~ 0.3 dex; and by Peterson, Kurucz, & Carney (1990), who find that two stars in M92 have [O/Fe] = 0.5, while the other α-elements are overabundant with respect to Fe by an amount of the order of 0.3–0.6 dex.

Although one could question, in principle, the reliability of any single result cited above, it is quite impressive that they all indicate a similar picture in which the α-elements (O included) are more or less equally overabundant with respect to Fe (by a factor which ranges, from author to author, between, say, 0.3 and 0.6 dex) and almost constant below [Fe/H] ~ -1.0. We should remark that the observed overabundance of the α-elements nicely matches the very basic theoretical (and intuitive) expectations that the first stars able to pollute the interstellar medium were the shortest living stars, i.e., the more massive ones which produce preferentially α-elements rather than iron (see, e.g., Matteucci & Greggio 1986).

The evidence that the α-elements are enhanced with respect to iron in metal-poor stars, coupled with the already-mentioned theoretical works showing that the evolutionary properties of the stellar models depend significantly on the adopted abundances of all the α-elements, strongly urges a revision of the "classical" models in order to take into account the detailed abundances of such elements (Tornambè 1987).

As far as we known, up to now the only models computed by taking into account the enhancement of most of the α-elements are the HB ones presented by Bencivenni et al. (1989) and widely used by Bencivenni et al. (1991).

In this paper, which is the third of a series of papers devoted to the production of updated isochrones useful for the study of the GGC system, we discuss the problem of the proper inclusion of the α-elements in the computation of low-metallicity, low-mass stellar models in a quite general way. In Paper I we described the latest version of our code—FRANEC—and made a comparison between our models and the others available in the literature. Paper II concerned the production of a extended set of "standard" theoretical isochrones and the analysis of 11 clusters by means of a new method we introduced (which was sketched in Paper I), which allows the determination of a cluster's age by means of the $(B-V)$ color difference between the TO and the base of the RGB. In the following, we present in § 2 some preliminary tests concerning the opacity effects of the elements other than H and He on the evolution of low-mass, low-metallicity stellar models, while the α-enhanced models and related isochrones are presented in § 3 together with their comparison with the standard scaled solar ones. The effect of the enhancement of the α-elements on the problem of the determination of the ages of the GGCs is addressed in § 4 by means of both the ΔV(HB − TO) and the $\Delta(B-V)$ methods, together with some comparisons with O-enhanced isochrones.

The main results of the present work have already been presented at several meetings (Chieffi, Straniero, & Salaris 1991; Straniero, Chieffi, & Salaris 1991a, b).

2. PRELIMINARY TESTS

All the evolutionary tracks described in this paper were obtained by means of our code FRANEC (an acronym for Frascati Raphson Newton Evolutionary Code), described in Paper I.

The computation of α-enhanced stellar models requires a proper evaluation of the influence of these elements (O, Ne, Mg, Si, S, and Ca) on both the burning and the opacity.

With regard to the first point, only the oxygen is important, because it enters in the CNO cycle. Its proper inclusion in the code is straightforward, since it is sufficient to redefine the oxygen abundance in the chemical composition of a given stellar model.

A proper computation of the opacity is much more difficult: the Los Alamos opacity library (Huebner et al. 1977) allows the computation of opacity tables for an arbitrary mixture only for temperatures higher than 12,000 K; below such a temperature we still have to rely on the available scaled solar opacity tables by Cox & Stewart (1979a, b) and Cox & Tabor (1976). By the way, since the two sets of tables merge at 12,000 K, for the sake of clarity in the following we will define the limiting temperature between the low (LTO) and high (HTO) temperature opacities as 12,000 K. In order to check quantitatively the influence of the metal content included in the LTO on the evolution of a stellar model, we compared evolutionary tracks (having the same mass, chemical composition, and HTO) computed by adopting LTOs of different metallicities. Hence, we evolved a standard 0.8 $M_\odot$ model ($Y = 0.23$; $Z = 10^{-4}$) after having substituted for the LTOs those for the metallicity $Z = 10^{-3}$. Figure 1*a* shows the evolutionary path of such a test model (*dashed line*) together with that of two standard models (*solid lines*) having the same mass and He abundance and metallicities $Z = 10^{-4}$ and $Z = 10^{-3}$; it is evident from the figure that the test model perfectly matches the path of the reference ($Z = 10^{-4}$) track through all the MS and TO regions, although the metal content in the LTO was increased by a factor of 10. On the contrary, as the test model approaches the RGB, it progressively overlaps the path of the standard model having $Z = 10^{-3}$. Other interesting properties of the test model are reported in Table 1: the H-burning lifetime (in Gyr), the logarithm of the luminosity (in solar units) of the RGB bump, the He core mass (in solar masses), the amount of He dredged to the surface as a consequence of the first dredge-up, the logarithm of the luminosity (in solar units), and the age (in Gyr) at the He flash. The first two rows refer to the standard tracks having $Z = 10^{-4}$ and $Z = 10^{-3}$, while the third one refers to the test model. Such a table clearly shows that the test model perfectly matches all the key evolutionary features of the reference ($Z = 10^{-4}$) track. Figure 1*b* shows a similar test performed this time on a 0.8 $M_\odot$ model ($Y = 0.23$; $Z = 10^{-3}$) which was evolved by adopting the LTO for the metallicity $Z = 10^{-4}$ (*dashed line*); the two solid lines represent the same standard models shown in Figure 1*a*. The fourth row in Table 1 reports the main evolutionary properties for this test model. It is evident that also in this case the metal content of the LTO does not play any significant role other than that of determining the location of the RGB. From these tests we can safely

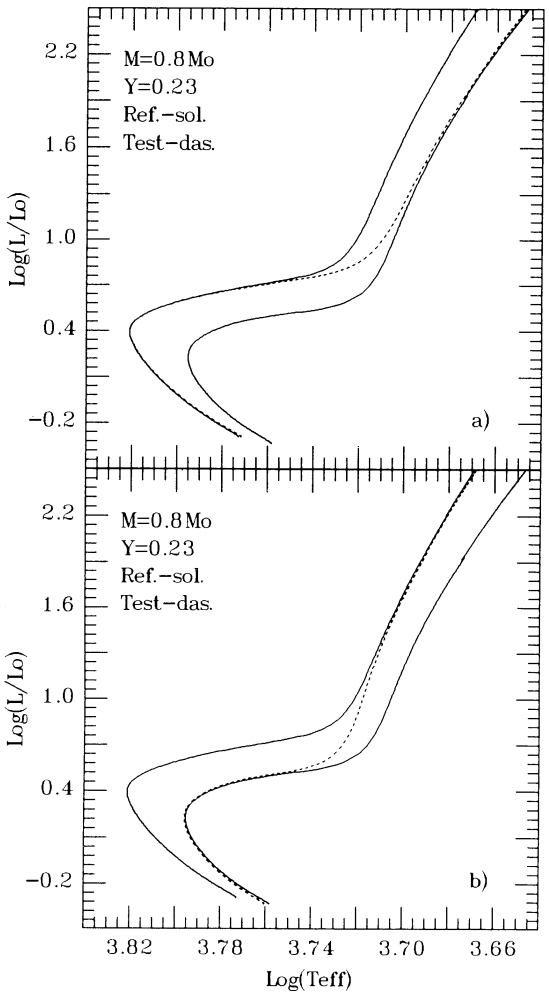

FIG. 1.—(*a*) Comparison among three evolutionary tracks concerning the evolution of a 0.8 $M_\odot$ model having $Y = 0.23$: the two solid lines refer to two standard models having metallicities $Z = 10^{-4}$ and $Z = 10^{-3}$, while the dashed line refers to the evolution of a model having $Z = 10^{-4}$ but computed by substituting for the opacity tables at temperatures lower than 12,000 K those for $Z = 10^{-3}$. (*b*) Same comparison as in (*a*): the dashed line refers in this case to the evolution of a model having $Z = 10^{-3}$ but computed by substituting for the opacity tables at temperatures lower than 12,000 K those for $Z = 10^{-4}$.

conclude that the lack of a proper inclusion of the overabundance of the α-elements in the computation of the LTO would only influence the location of the RGB. Such a feature is in any case subject to serious uncertainties due to, for example, the still poor treatment of the convection in the superadiabatic layers and to the $(B-V)$–$T_{\rm eff}$ relation, which is of crucial importance when comparing theoretical H-R diagrams to the observed ones (see Paper II).

Let us now show the opposite test, i.e., the influence of the metal content included in the HTO on the evolution of a stellar model. Figure 2*a* shows the evolutionary track of a 0.8 $M_\odot$, $Y = 0.23$, $Z = 10^{-4}$ model (*dashed line*), computed by adopting the HTO for the metallicity $Z = 10^{-3}$; the two solid lines are the two standard tracks already shown in the previous figure. In this case the test model behaves like the standard $Z = 10^{-3}$ all along the MS and has a TO luminosity intermediate between the two standard tracks, while the RGB closely follows that of the reference ($Z = 10^{-4}$) stellar model. Such a test shows that the metal content included in the HTO dominates in determining the MS location; it significantly influences the TO luminosity, while it does not affect the position of the RGB. A similar test was also performed on a stellar model having $Z = 10^{-3}$ but the HTO for the metallicity $Z = 10^{-4}$. The results are in total agreement with the ones discussed above and are shown in Figure 2*b*. The fifth and sixth rows in Table 1 report the main evolutionary properties of these test models. Such quantities differ significantly from those obtained for the corresponding reference tracks: this means that they are affected by the metal content included in the HTO. In particular, (*a*) the H-burning lifetime of each of these two models is closer to that of the standard model having the same HTO rather than to that of the parent reference track (this is due to the fact that each of these two test models closely matches the luminosity of the reference track having the same HTO all along the MS and the TO); (*b*) the luminosities of the RGB bump and the extra He brought to the surface as a consequence of the first dredge-up episode are intermediate between those obtained for the two reference models (which means that both the metal content included in the HTO and the amount of the CNO nuclei affect these quantities); and (*c*) the He core masses at the He flash are similar to the ones obtained for the parent reference tracks (since this value mainly depends on the amount of the CNO nuclei).

All these tests may be summarized by stating that the MS and TO locations of a star model in the H-R diagram, the MS and RGB lifetimes, the RGB bump luminosity, the He core mass at the He flash, the extra He brought to the surface by the

TABLE 1

MAIN EVOLUTIONARY PROPERTIES OF THE MODELS EVOLVED UP TO THE He FLASH

$M = 0.8\ M_\odot$, $Y = 0.23$ (1)	t_9(H) (2)	$L_{\rm bump}$ (3)	M_c (4)	δY (5)	$L_{\rm FL}$ (6)	t_9(FL) (7)
$Z = 10^{-4}$–standard	14.20	2.21	0.511	0.008	3.28	15.10
$Z = 10^{-3}$–standard	15.24	1.92	0.500	0.013	3.36	16.51
$Z = 10^{-4}$–κ(LTO) = $Z = 10^{-3}$	14.21	2.21	0.511	0.008	3.28	15.11
$Z = 10^{-3}$–κ(LTO) = $Z = 10^{-4}$	15.25	1.93	0.500	0.013	3.36	16.51
$Z = 10^{-4}$–κ(HTO) = $Z = 10^{-3}$	15.76	2.04	0.513	0.010	3.29	16.80
$Z = 10^{-3}$–κ(HTO) = $Z = 10^{-4}$	13.71	2.11	0.498	0.011	3.36	14.84
$Z = 10^{-4}$–[α/Fe] = 0.6	14.37	2.11	0.506	0.010	3.32	15.40
$Z = 10^{-3}$–[α/Fe] = 0.6	17.84	1.73	0.496	0.014	3.40	19.54
$Z = 2.91 \times 10^{-4}$–standard	14.36	2.11	0.506	0.010	3.32	15.38
$Z = 2.91 \times 10^{-3}$–standard	17.75	1.70	0.496	0.015	3.40	19.47

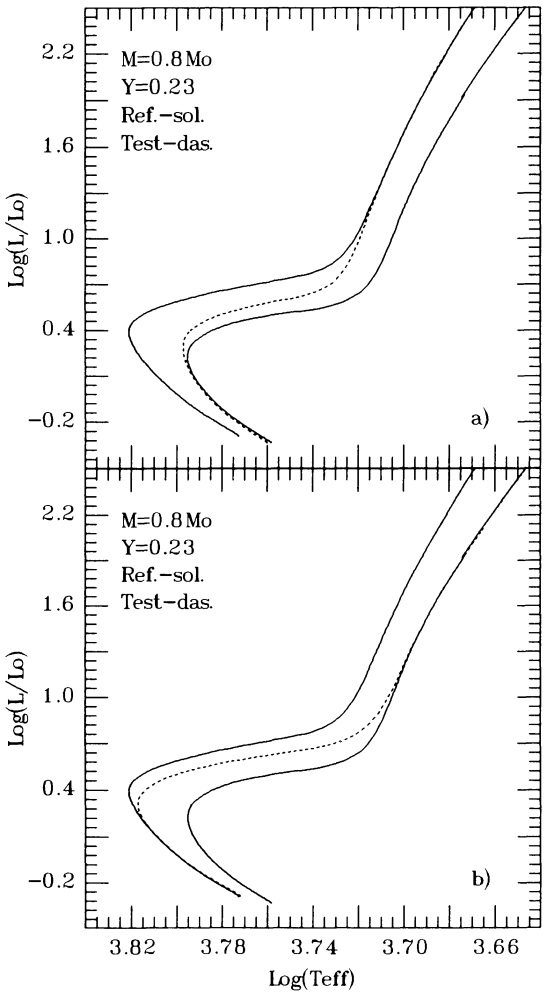

FIG. 2.—Solid lines refer to the same star models described in Fig. 1. The dashed line in (*a*) refers to the evolution of a model having $Z = 10^{-4}$ but computed by substituting for the opacity tables at temperatures higher than 12,000 K those for $Z = 10^{-3}$, while in (*b*) it refers to the evolution of a model having $Z = 10^{-3}$ but computed by substituting for the opacity tables at temperatures higher than 12,000 K those for $Z = 10^{-4}$.

first dredge-up, and the luminosity at the tip of the RGB depend on both the metal content included in the opacities adopted at temperatures larger than 12,000 K and on the amount of CNO nuclei, while they turn out to be insensitive to the metal content included in the opacities at temperatures lower than 12,000 K. On the contrary, the location of the RGB depends on the metal content included in the LTO and not on that included in the HTO or on the abundance of the CNO nuclei.

3. THE α-ENHANCED MODELS AND RELATED ISOCHRONES

3.1. *The H-burning Phase*

Let us first analyze the MS and TO regions, since these evolutionary phases are not influenced by the metal content included in the LTO. For the sake of clarity, let us mention that we adopted the standard Cox & Stewart (1970a, b) and Cox & Tabor (1976) opacity tables below 12,000 K. The basic solar mixture we adopted is the Ross-Aller (1976) mix, in order to remain fully compatible with our previous computations (Papers I and II). However, we will show in the following that the adoption of an updated set of solar abundances has a totally negligible effect on our results. Table 2 lists the elements heavier than He and related abundances (normalized to unity), as given by Ross & Aller, in columns (1) and (2). All the abundances in the present table are in mass fraction.

Since the available observational data concerning the abundances of the α-elements in metal-poor stars show that, for each given iron abundance, all the α-elements are similarly enhanced (see above) and that an overabundance of 0.6 dex may be considered a fair upper limit, let us start the analysis by adopting an equal overabundance by a factor of 4 for all the α-elements. Column (3) in Table 2 shows the abundances of the elements included in the Ross-Aller mixture once the abundances of the α-elements O, Ne, Mg, Si, S, and Ca are increased by a factor of 4. The last row in the table shows the factor f which connects a given scaled solar metallicity Z_0 to the global metallicity Z (i.e., the one including the overabundances of the given elements). Appropriate opacity tables for this chemical composition were obtained by means of the Los Alamos opacity library.

Figures 3 and 4 show the evolutionary path of three selected stellar models having masses equal to 0.6, 0.8, and 1.0 $M_\odot$, $Y = 0.23$, and the same metallicity; Figure 3 refers to the scaled solar metallicity $Z_0 = 10^{-4}$ and Figure 4 to $Z_0 = 10^{-3}$. The solid lines represent the standard reference tracks while the dashed ones are for the α-enhanced models. Let us first discuss the models having $Z_0 = 10^{-3}$. The proper inclusion of all the α-elements shifts the star models toward the red and reduces their TO luminosity with respect to the "standard" models. Such a behavior is comprehensible, since the enhancement of the α-elements increases both the CNO burning (which affects the departure of a stellar model from the MS) and the opacity (which determines the total amount of energy required to sustain a star and its radius). The models having $Z_0 = 10^{-4}$ show a qualitatively similar picture, but, since the overall metallicity is much lower, the differences are in this case quantitatively smaller.

TABLE 2

ABUNDANCES BY MASS FRACTION OF THE VARIOUS MIXTURES DESCRIBED IN TEXT

Element (1)	Ross-Aller (2)	α × 4 (3)	α × 8 (4)
C	0.21785	0.2179	0.2179
N	0.05308	0.0531	0.0531
O	0.48158	1.9263	3.8526
Ne	0.03262	0.1305	0.2610
Na	0.00190	0.0019	0.0019
Mg	0.04211	0.1684	0.3369
Al	0.00390	0.0039	0.0039
Si	0.05458	0.2183	0.4366
P	0.00043	0.0004	0.0004
S	0.02210	0.0884	0.1768
Cl	0.00049	0.0005	0.0005
Ar	0.00175	0.0018	0.0018
Ca	0.00391	0.0156	0.0313
Ti	0.00023	0.0002	0.0002
Cr	0.00115	0.0012	0.0012
Mn	0.00063	0.0006	0.0006
Fe	0.07684	0.0768	0.0768
Ni	0.00485	0.0049	0.0049
f	1.00000	2.9107	5.4583

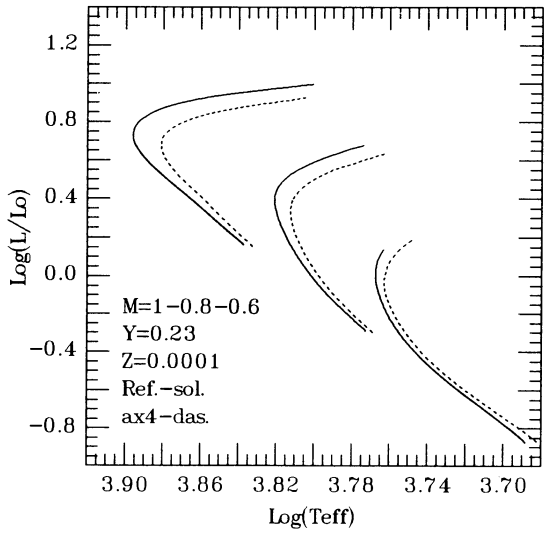

FIG. 3.—Comparison between standard scaled solar models (*solid lines*) having masses equal to 1, 0.8, and 0.6 $M_\odot$ ($Y = 0.23$ and $Z_0 = 10^{-4}$) and models obtained by enhancing the α-elements O, Ne, Mg, Si, S, Ca by a factor of 4 (*dashed lines*).

By means of the models discussed above, complemented by two further masses (i.e., 0.9 and 0.7 $M_\odot$), we have also computed "enhanced" sets of isochrones for both metallicities, in the age range 10 Gyr $\leq t \leq$ 20 Gyr. Figures 5 and 6 show, for the two metallicities $Z_0 = 10^{-4}$ (Fig. 5) and $Z_0 = 10^{-3}$ (Fig. 6), two selected-isochrones having ages equal to, respectively, 12 and 18 Gyr. Also in this case, the solid and dashed lines refer, respectively, to the standard and α-enhanced isochrones. Quite obviously, the α-enhanced isochrones reflect the properties of the respective evolutionary star models. From both figures it can be seen that an overabundance of the α-elements shifts the MS toward the red and dims the TO luminosity. Once again let us remark that such effects depend on the metallicity, in the sense that they grow as the overall metallicity increases. In order to quantify the effect of the enhancement of the α-

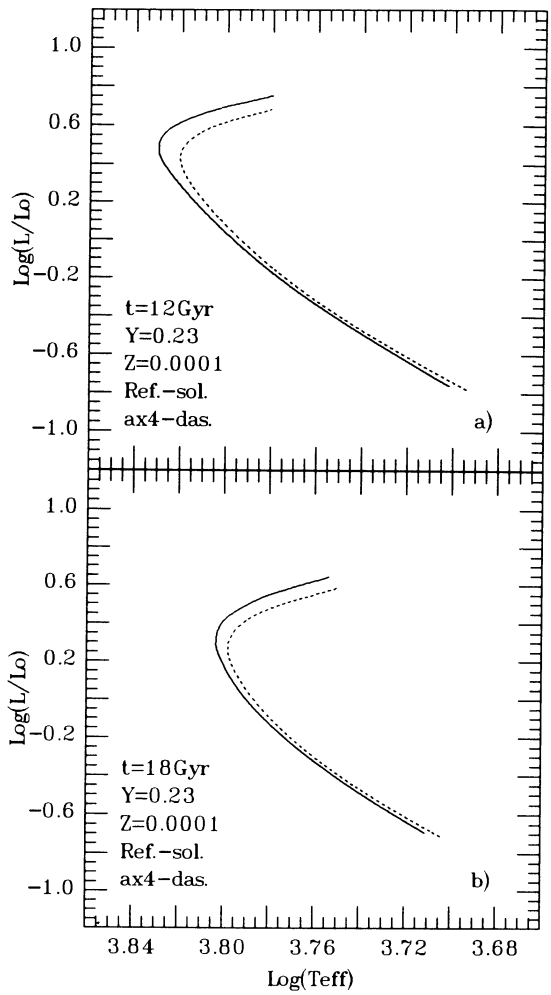

FIG. 5.—Comparison between a standard scaled solar isochrone (*solid line*) having $Y = 0.23$ and $Z_0 = 10^{-4}$ and the isochrone of the same age obtained by enhancing the α-elements by a factor of 4 (*dashed line*). (*a*) = 12 Gyr; (*b*) = 18 Gyr.

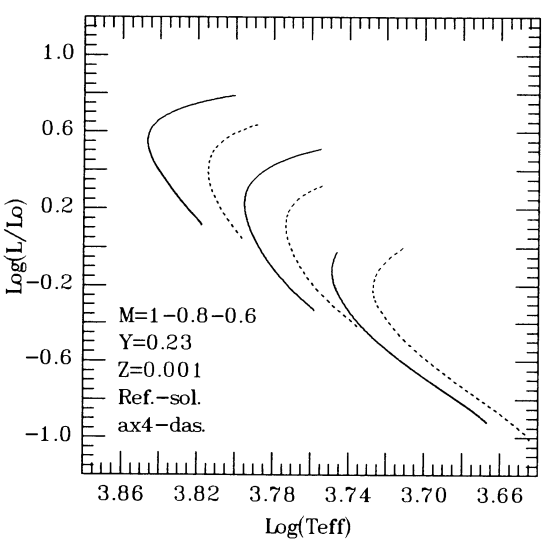

FIG. 4.—Same comparison as in Fig. 3, but for $Z_0 = 10^{-3}$

elements by a factor of 4, we plotted in Figure 7, for the two quoted reference metallicities $Z_0 = 10^{-4}$ and $Z_0 = 10^{-3}$, the TO visual magnitude as a function of the age for the standard (*solid line*) and α-enhanced (*dashed line*) isochrones. The increase of the α-elements by 0.6 dex leads to an age reduction by $\sim$2 Gyr at $Z_0 = 10^{-4}$ and by $\sim$2.5 Gyr at $Z_0 = 10^{-3}$. Of course, the TO visual magnitude is not the only parameter of interest. Another quantity which is worth deriving is the $(B-V)$ MS location as a function of the metallicity. From the standard isochrones we obtain that the MS scales, at $M_v = 6$, between $Z_0 = 10^{-4}$ and $Z_0 = 10^{-3}$, as

$$\frac{\Delta(B-V)_{MS}}{\Delta \log Z} = 0.067 ,$$

while the α-enhanced isochrones scale as

$$\frac{\Delta(B-V)_{MS}}{\Delta \log Z} = 0.97 ,$$

which means a consistent increase of the scaling of the MS as a function of the metallicity. It goes without saying that the

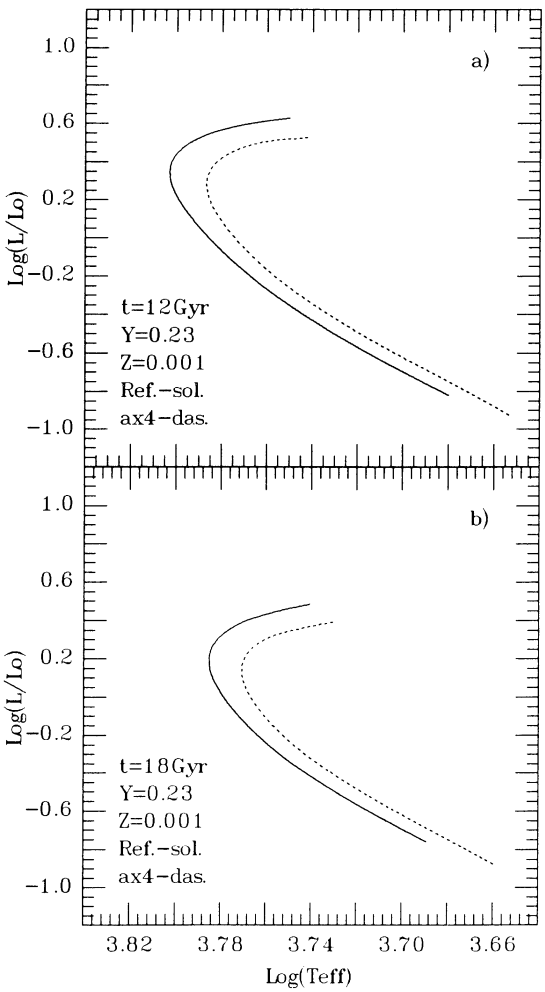

FIG. 6.—Same comparison as in Fig. 5, but for $Z_0 = 10^{-3}$

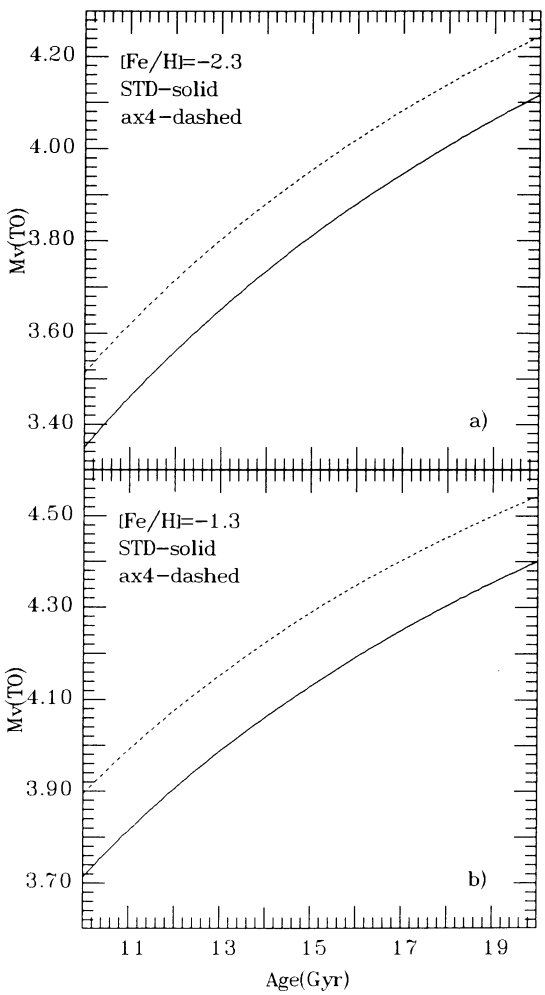

FIG. 7.—Visual magnitude of the TO as a function of age: the solid line refers to the standard scaled solar case, while the dashed line refers to the case in which the α-elements are enhanced by a factor of 4. The two panels refer, respectively, to the metallicities (*a*) $Z_0 = 10^{-4}$ (*b*) $Z_0 = 10^{-3}$.

transformations adopted here in order to transform the isochrones from the theoretical plane to the observational one are the same as those adopted in Paper II.

In addition to the two relations described above, it is also of great importance to determine the influence of the α-elements on the bump luminosity, on the RGB, on the efficiency of the first dredge-up, on the He core mass at the He flash, and on the visual magnitude of the tip of the RGB. By the way, let us remind the reader that we have already demonstrated in the previous section that none of these quantities depends on the metal content included in the LTO. For such a reason we prolonged the evolution of the two "α-enhanced" models, for 0.8 $M_\odot$ and the metallicities quoted above, up to the He flash. Table 1 shows the main features of these evolutionary tracks in rows 7 and 8.

Up to now we have compared the enhanced models, and associated isochrones, with the standard nonenhanced models. However, since the enhancement of one or more elements increases the global metallicity of the model, it is interesting to compare the enhanced models with the standard ones of the same global metallicity Z, in order to make evident the differences in the evolutionary properties which arise from the different relative distribution of the elements once the total metallicity Z is fixed.

The enhancement of the α-elements by a factor of 4 above a given scaled solar metallicity Z_0 implies an overall increase of the metallicity by a factor $f = 2.91$ ($Z = 2.91 Z_0$; see Table 2), and hence we compare, in Figures 8 and 9, the α-enhanced models (*solid lines*) with the respective standard ones (*dashed lines*) having $Z_0 = 2.91 \times 10^{-4}$ and $Z_0 = 2.91 \times 10^{-3}$ (appropriate opacity tables have been computed for these two metallicities), while the comparison between the respective isochrones for the two ages 12 and 18 Gyr is shown in Figures 10 and 11. A look at these figures shows, quite surprisingly, that the two sets of models (and relative isochrones) coincide almost perfectly. Moreover, the two enhanced models evolved up to the He flash clearly show that the evolutionary properties of the RGB phase also coincide almost perfectly (see Table 1, rows 9 and 10). It follows that the evolutionary features of an α-enhanced stellar model are determined essentially by the global metallicity and not by the relative abundances of the various elements.

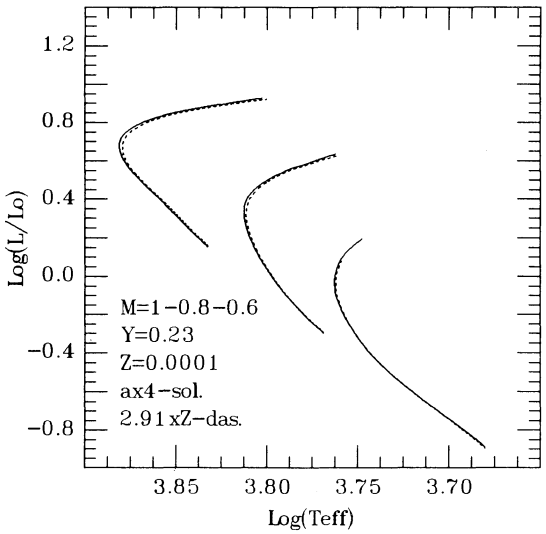

FIG. 8.—Comparison between standard scaled solar models (*dashed lines*) having masses equal to 1, 0.8, and 0.6 $M_\odot$ ($Y = 0.23$ and $Z_0 = 2.91 \times 10^{-4}$) and models obtained by enhancing the α-elements by a factor of 4 (*solid lines*) above the scaled solar metallicity $Z_0 = 10^{-4}$.

In order to check whether such a result was due to the particular choice of enhancement factor, we recomputed two sets of models with the α-elements enhanced by a factor of 8. In such cases the global metallicity is increased by a factor $f = 5.46$ (see Table 2, col. [4]), and therefore these enhanced models must be compared with the standard ones having metallicities $Z_0 = 5.46 \times 10^{-4}$ and $Z_0 = 5.46 \times 10^{-3}$, respectively; such a comparison is shown in Figures 12 and 13 for the two metallicities, where the solid and dashed lines represent the enhanced and standard models, respectively. It is evident also in this more extreme case that the good match between the two sets of models indicates that the α-enhanced models are quite well simulated by the standard ones having the same global metallicity. In order to shed some light on these unexpected

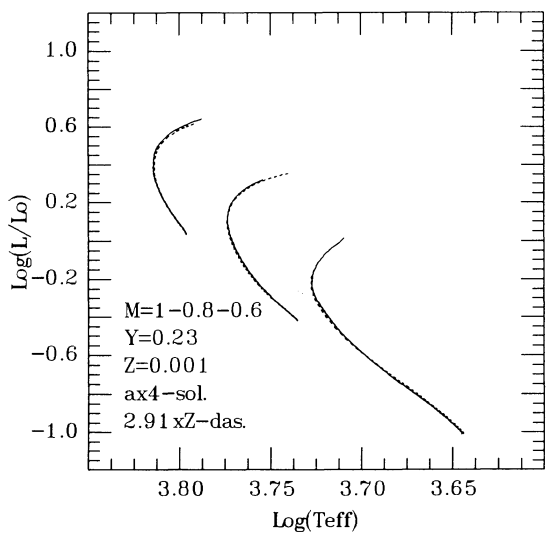

FIG. 9.—Comparison between standard scaled solar models (*dashed lines*) having masses equal to 1, 0.8, and 0.6 $M_\odot$ ($Y = 0.23$ and $Z_0 = 2.91 \times 10^{-3}$) and models obtained by enhancing the α-elements by a factor of 4 (*solid lines*) above the scaled solar metallicity $Z_0 = 10^{-3}$.

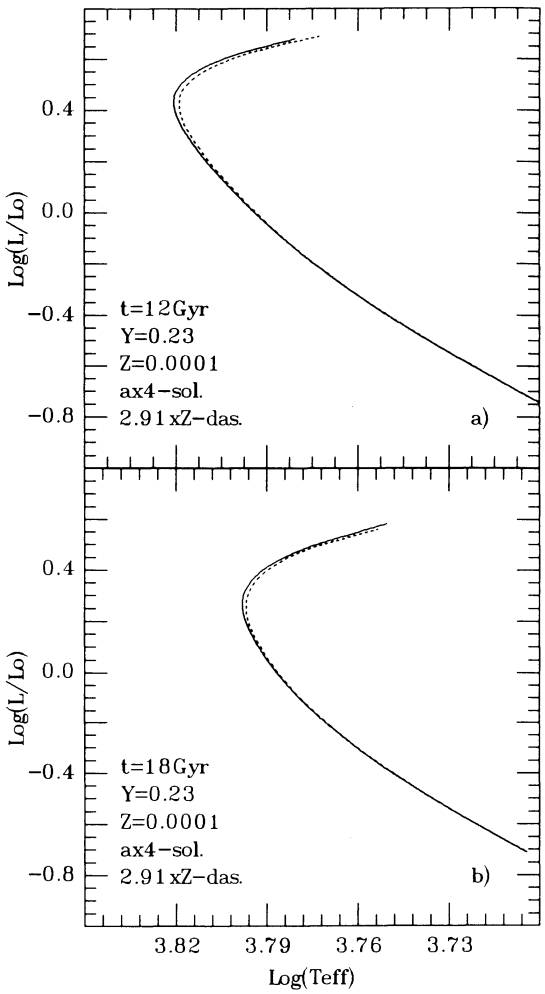

FIG. 10.—Comparison between a standard scaled solar isochrone (*solid line*) having $Y = 0.23$ and $Z_0 = 2.91 \times 10^{-4}$ and the isochrone obtained by enhancing the α-elements by a factor of 4 (*dashed* line) above the scaled solar metallicity $Z_0 = 10^{-4}$. The two cases corresponding to the ages 12 and 18 Gyr are shown in (*a*) and (*b*), respectively.

results, we have to consider the contributions of the individual chemical species to both the burning and the opacity.

The efficiency of the CNO burning is controlled by the total abundance, by number, of these three elements. Hence the efficiency of the CNO burning in a star model in which the abundances by number of X_C, X_N, and X_O are altered with respect to the scaled solar values coincides with that of the model having a scaled solar metallicity $Z' = f_{CNO} Z_0$, where the factor f_{CNO} equals

$$f_{CNO} = \frac{X_C + X_N + X_O}{X_C^0 + X_N^0 + X_O^0},$$

and X_C^0 (=0.3028), X_N^0 (=0.0633), and X_O^0 (=0.5025) represent the scaled solar values and Z_0 the starting (unaltered) metallicity. For example, if the O abundance is increased by a factor of 2 in a star model having initially a scaled solar metallicity Z_0, the factor f_{CNO} equates to 1.58, and therefore the CNO burning of the enhanced model equals that of a model having a scaled solar metallicity $Z' = 1.58 Z_0$.

Concerning the contributions of the various elements to the global opacity, the situation is much more complex, since it is

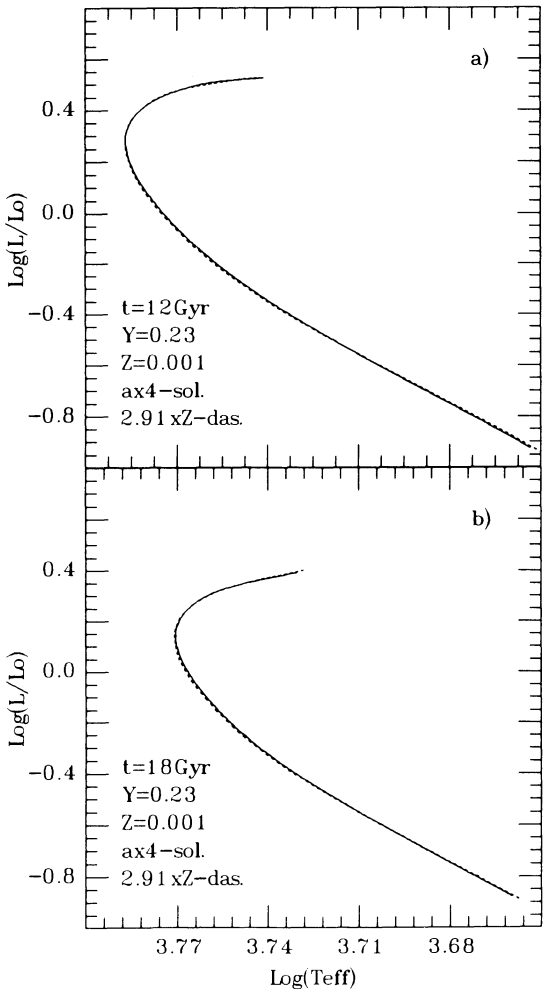

FIG. 11.—Comparison between a standard scaled solar isochrone (*solid line*) having $Y = 0.23$ and $Z_0 = 2.91 \times 10^{-3}$ and the isochrone obtained by enhancing the α-elements by a factor of 4 (*dashed line*) above the scaled solar metallicity $Z_0 = 10^{-3}$. The two cases corresponding to the ages of 12 and 18 Gyr are shown, in (*a*) and (*b*) respectively.

not evident, and in general certainly not true, that, analogous to the CNO burning, the opacity depends on the global rather than the individual abundances of the various chemical species. By the way, we note that the tests we will discuss in what follows concern the comparison of evolutionary tracks and not directly of opacity tables; this means that we analyze the effect of the opacity only in that part of the (T, ρ)-plane which is crossed by these models, and therefore the present results may not necessarily be valid for masses outside the range discussed here or for other evolutionary phases.

A look at the solar mixture (either the Ross-Aller mixture or a more recent one, e.g., Grevesse 1984; Meyer 1985; Anders & Grevesse 1989) shows that C, N, and Fe plus the α-elements O, Ne, Mg, Si, S, and Ca account for ≈99% in mass of the total metallicity Z. A second thing to note is that five out of these nine elements, i.e., Mg, Si, S, Ca, and Fe, have similarly low first-ionization potentials. Therefore, one could suspect that they behave similarly as opacity sources (as already suggested by Iben 1965 and Renzini 1977). In order to check such a possibility, we prepared opacity tables for two special mixtures: the first was obtained by enhancing only O and Ne by a

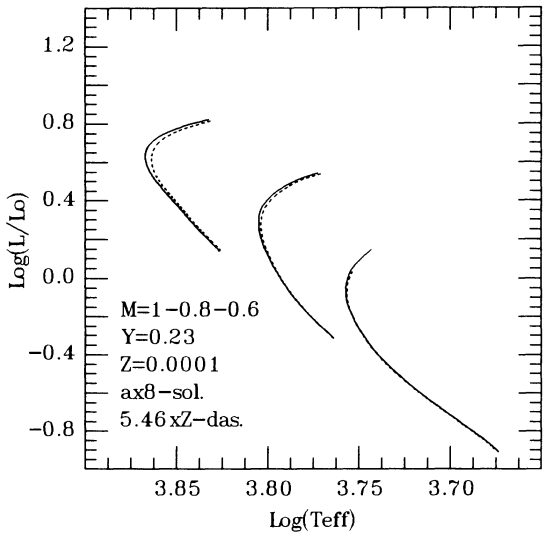

FIG. 12.—Comparison between standard scaled solar models (*dashed lines*) having masses equal to 1, 0.8, and 0.6 $M_\odot$ ($Y = 0.23$ and $Z_0 = 5.46 \times 10^{-4}$) and models obtained by enhancing the α-elements by a factor of 8 (*solid lines*) above the scaled solar metallicity $Z_0 = 10^{-4}$.

factor of 4, and the second by enhancing O, Ne, and Fe—the first two elements by the usual factor of 4 and the Fe by an amount equal to the sum of the overabundances by mass which should be attributed separately to Mg, Si, S, and Ca, were they individually enhanced by a factor of 4 [i.e., $X_{Fe} = 4(X^0_{Mg} + X^0_{Si} + X^0_S + X^0_{Ca}) + X^0_{Fe}$]. Using these opacity tables, we have evolved a 0.8 $M_\odot$ ($Y = 0.23$ and $Z_0 = 10^{-3}$) model. Figure 14 shows the results of such a test: the long-dashed line represents the standard evolutionary track, the dashed line the one obtained by enhancing only O and Ne, the dotted line the one obtained by enhancing O, Ne, and Fe, while the solid one shows the "standard" α-enhanced model. Let us first note that the existing difference between the dashed (O- and Ne-enhanced) and the solid (α-enhanced) lines quantitatively

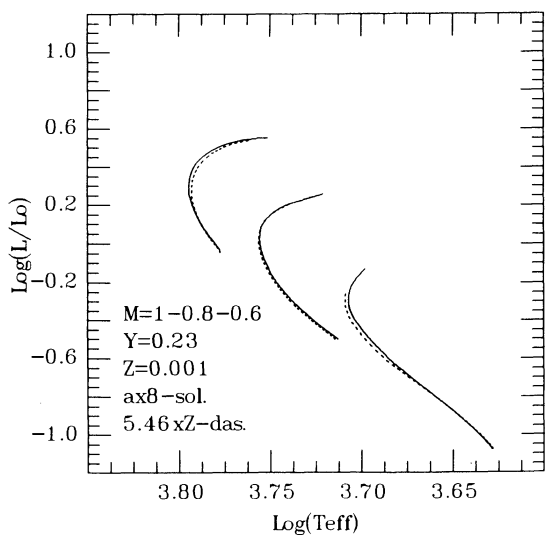

FIG. 13.—Comparison between standard scaled solar models (*dashed lines*) having masses equal to 1, 0.8, and 0.6 $M_\odot$ ($Y = 0.23$ and $Z_0 = 5.46 \times 10^{-3}$) and models obtained by enhancing the α-elements by a factor of 8 (*solid lines*) above the scaled solar metallicity $Z_0 = 10^{-3}$.

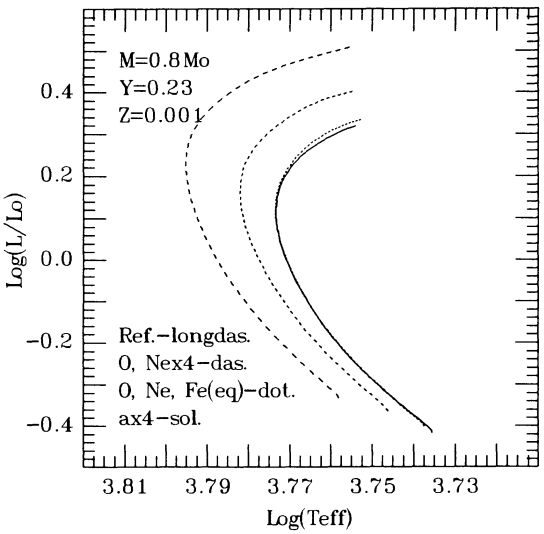

FIG. 14.—Influence of various chemical species on the evolution of a 0.8 $M_\odot$ model having $Y = 0.23$ and metallicity $Z_0 = 10^{-3}$. The long-dashed line refers to the standard scaled solar model, the dashed line refers to the case in which O and Ne are enhanced by a factor of 4, the solid line refers to the model obtained by enhancing all the α-elements (O, Ne, Mg, Si, S, and Ca) by a factor of 4, while the dotted line refers to the case in which O and Ne are enhanced by a factor of 4 and the Fe abundance was set equal to $X_{Fe}(\text{new}) = X_{Fe} + 3(X_{Mg} + X_{Si} + X_S + X_{Ca})$; see text.

shows the global influence of Mg, Si, S, and Ca on the evolutionary path of the stellar model. Second, the extremely good match between the "standard" α-enhanced (*solid lines*) and the O-, Ne-, and Fe-enhanced (*dotted lines*) stellar models clearly proves that a star model reacts essentially to the global abundance of these elements and not to their individual abundances. Note that both axes are intentionally greatly expanded. It follows that the evolutionary properties of a star model of initial metallicity Z_0 in which some of these elements (Mg, Si, S, and Ca) are enhanced with respect to their scaled solar values may be obtained by adopting the standard metallicity Z'' having the same global abundance of these elements. The rescaling factor f_{LPE} is given by:

$$f_{LPE} = \frac{X_{Mg} + X_{Si} + S_S + X_{Ca} + X_{Fe}}{X^0_{Mg} + X^0_{Si} + X^0_S + X^0_{Ca} + X^0_{Fe}},$$

where the superscript zero indicates the scaled solar values and LPE stands for "low-potential elements." The equivalent metallicity Z'' is given by

$$Z'' = f_{LPE} Z_0 .$$

The remaining elements, i.e., C, N, O, and Ne, do not have similar first-ionization potentials, and hence there is no reason to think that they will behave similarly as opacity sources. In order to make evident the global contribution of C, N, and Ne, we prepared opacity opacity tables in which the abundances of these elements were simply zeroed. Note that we zeroed these elements only for the computation of the opacity tables and *not* for the determination of the CNO burning. The evolution of a 0.8 $M_\odot$, $Y = 0.23$, and $Z_0 = 10^{-3}$ model computed by adopting these special opacities is shown in Figure 15 as a dotted line, together with the standard model (*solid line*): the difference between the two lines clearly shows that the three elements influence the evolutionary path of the stellar model and hence they cannot be neglected. As a second test, we wanted to evaluate the error which would result from treating these four elements as equivalent. Hence we prepared opacity tables by assuming an O abundance equal to the sum of the abundances by mass of C, N, O, and Ne ($X_O = X^0_C + X^0_N + X^0_O + X^0_{Ne}$), while the individual abundances of C, N and Ne were zeroed again. Figure 15 shows the resulting evolutionary track as a dashed line: it is evident that such a track coincides almost perfectly with the standard reference one. It follows that, contrary to what one could expect a priori, these elements constitute a group in the sense that only their global abundance by mass enters in determining their contribution to the opacity, at least within the range of masses and evolutionary phases of interest for the present paper. Once again we can say that the evolution of a stellar model in which one or more of these elements have nonscaled solar abundances coincides with the standard reference model having the metallicity $Z''' = f_{HPE} Z_0$, where the factor f_{HPE} is given by

$$f_{HPE} = \frac{X_C + X_N + X_O + X_{Ne}}{X^0_C + X^0_N + X^0_O + X^0_{Ne}},$$

where HPE stands for "high potential elements."

From all these tests concerning the influence of the various elements on the opacity, we can summarize the following results: the nine most abundant elements in the solar mixture may be divided into two distinct groups, as opacity sources: the first includes C, N, O, and Ne, while the second includes Mg, Si, S, Ca, and Fe. The individual elements within each group do not have a specific signature on the evolutionary path of the stellar model (within the range of masses and metallicities studied here), but, instead, they behave in a similar way, so that only the total abundance by mass of the elements within each group is important in determining the evolutionary path of the star model. It follows, therefore, that, whatever the enhancement for each individual chemical species, if the

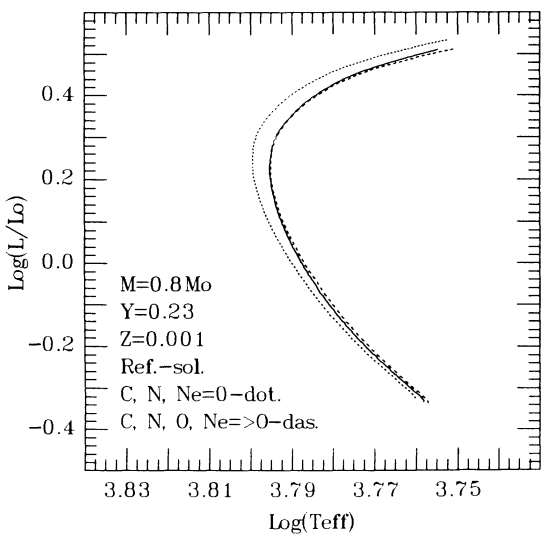

FIG. 15.—Influence of various chemical species on the evolution of a 0.8 $M_\odot$ model having $Y = 0.23$ and metallicity $Z_0 = 10^{-3}$. The solid line refers to the standard scaled solar model, the dotted line refers to the case in which the adopted opacities were computed by adopting a mixture in which the abundances of C, N, and Ne were zeroed while the dashed line refers to the case in which the opacity tables were obtained by adopting a mixture in which the abundance of the O increased by adding the individual abundances of C, N, and Ne, and these three elements zeroed again; see text.

two average enhancing factors $f_{\rm HPE}$ and $f_{\rm LPE}$ are similar, then one can identify a unique average enhancing factor

$$f_\kappa = f_{\rm HPE} \simeq f_{\rm LPE} ,$$

which simply means that there exists a standard scaled solar metallicity Z whose opacity resembles that obtained by enhancing the α-elements above a given metallicity Z_0. Such a metallicity is simply obtained by means of the factor f_κ:

$$Z = f_\kappa Z_0 .$$

If we now combine the results obtained for the opacity and the burning, it becomes clear that, if $f_{\rm CNO} \simeq f_\kappa$ ($\simeq f_{\rm HPE} \simeq f_{\rm LPE}$), then there exists a standard scaled solar metallicity Z which resembles in every respect the α-enhanced one. Such a metallicity may be obtained as

$$Z = \bar{f}(\simeq f_{\rm CNO} \simeq f_\kappa) Z_0 .$$

It is worth noting that since in practice $f_{\rm HPE}$ is always similar to $f_{\rm CNO}$ because $X_{\rm Ne}$ is always much smaller than the sum of $X_{\rm C} + X_{\rm N} + X_{\rm O}$, the only condition which must be verified for the existence of a unique rescaling factor reduces to

$$f_{\rm HPE} \simeq f_{\rm LPE} .$$

Such a condition may be also written as

$$\left[\frac{X_{\rm C} + X_{\rm N} + X_{\rm O} + X_{\rm Ne}}{X_{\rm Mg} + X_{\rm Si} + X_{\rm S} + X_{\rm Ca} + X_{\rm Fe}}\right] \equiv \left[\frac{X_{\rm HPE}}{X_{\rm LPE}}\right] \simeq 0 ,$$

where the square brackets have the usual meaning, i.e. $[A/B] \equiv \log (A/B)_* - \log (A/B)_\odot$. Moreover, if this condition is verified, then this unique rescaling factor practically coincides with the factor f by which the nonenhanced metallicity must be multiplied in order to get the global one:

$$Z_{\rm GLOB} = f Z_0 .$$

Such an occurrence is trivially due to the fact that the nine elements (C, N, O, Ne, Mg, Si, S, Ca, and Fe) constitute more than the 99% by mass of the metallicity. By means of a linear regression through the enhancement factors "f" which correspond to different enhancement factors "f_α" of the α-elements, one may derive the general relation

$$f = 0.638 f_\alpha + 0.362 ,$$

which connects the enhancement of the α-elements to the enhancement of the global metallicity. For example, an enhancement of the α-elements by a factor $f_\alpha = 4$ implies an enhancement of the global metallicity by a factor $f = 2.91$. The adoption of a more recent solar mixture would not alter significantly the relation given above. For example, if one would adopt as the solar mixture that quoted by Grevesse (1984), Meyer (1985), or Anders & Grevesse (1989), the enhancement of the α-elements by a factor of 4 would imply an enhancement of the global metallicity by a factor f ranging between 2.86 and 3.02, values very close to the one (2.91) obtained for the Ross-Aller mixture.

At this point the good match between α-enhanced and standard models having the same global metallicity (shown at the beginning of this section) becomes perfectly comprehensible. In fact, the α-enhanced models (by a factor of 4) coincide with the standard ones of similar total metallicity because $[X_{\rm HPE}/X_{\rm LPE}] = 0.02$ $[f(=2.91) \simeq f_{\rm HPE}(=2.97) \simeq f_{\rm LPE}(=2.85) \simeq f_{\rm CNO}(=2.74)]$; the same is true for the case in which the α-elements were enhanced by a factor of 8: $[X_{\rm HPE}/X_{\rm LPE}] = 0.02$ $[f(=5.46) \simeq f_{\rm HPE}(=5.58) \simeq f_{\rm LPE}(=5.48) \simeq f_{\rm CNO}(=5.05)]$.

The last feature which remains to be analyzed is the effect of the enhancement of the α-elements on the location of the RGB. Unfortunately, this is totally determined by the LTO, and hence it is not possible to analyze the separate contributions of the individual elements to the opacity. However, since it has long been recognized (Iben 1965; Renzini 1977; VandenBerg 1992) that the main contributors to the LTO are the elements having similarly low first-ionization potentials, i.e., Mg, Si, S, Ca, and Fe, because they are the main electron donors, and since we have checked that such an occurrence is valid above 12,000 K, we assume that the five elements Mg, Si, S, Ca, and Fe constitute a group (in the sense that the opacity depends only on the global abundance of such elements and not on the specific abundance of each of them) also below 12,000 K. It goes without saying that we are totally neglecting the contribution of the α-elements to the formation of the molecules: however, it must be said that the lack of a proper inclusion of the contribution of the molecules to the opacity also concerns the standard opacity, and hence it must be considered as one of the general uncertainties which affect, at present, the computation of all the stellar models.

Anyway, with such an assumption concerning the location of the RGB, we obtain the result that, provided that $[X_{\rm HPE}/X_{\rm LPE}] \simeq 0$, all the properties of the α-enhanced isochrones may be obtained by a simple rescaling of the metallicity.

While we were writing this paper, we received a preprint by Chaboyer, Sarajedini, & Demarque (1992, hereafter CSD92) concerning the computation of a set of α-enhanced models: among other things, the authors checked the present results, which had already been briefly described in Chieffi et al. (1991), and found the α-enhanced models to coincide remarkably with the standard models having the same global metallicity.

Let us comment briefly on how the picture would change if the overabundance of one of the α-elements (e.g., the oxygen) were larger than that of the other α-elements (i.e., if $[X_{\rm HPE}/X_{\rm LPE}]$ were very different from zero). In such a case it would be necessary actually to compute enhanced models; however, if such an "over"-overabundance remained within, say, a factor of 2, then the differences between the "enhanced" and rescaled isochrones would not be very serious. In fact, let us imagine that at a given metallicity Z_0 a given α-element was overabundant by a factor of 8 while the other α-elements were enhanced by a factor of 4. In such a case the enhancement by a factor of 4, common to all the α-elements, could be taken into account by adopting the standard isochrones having a metallicity $Z = 2.91 Z_0$, and hence the initial overabundance by a factor of 8 of that α-element with respect to the initial metallicity Z_0 would be reduced to a much smaller amount, i.e., a factor of 2, with respect to the rescaled metallicity Z.

Before closing this section we want to show a further check which shows that the opacity of a given mixture may be obtained by assuming a mixture made only by O and Fe (representative of the two opacity groups identified above). In particular, we decided to verify whether the standard evolutionary tracks having the scaled solar metallicities $Z_0 = 10^{-4}$ and $Z_0 = 10^{-3}$ could be reproduced by models computed by substituting for standard opacity tables those obtained by assuming a mixture formed by only O and Fe having abun-

dances by mass (normalized to unity) equal to

$$X_O = 0.797 \quad [\equiv (X_C^0 + X_N^0 + X_O^0 + X_{Ne}^0)/X_{TOT}^0] ,$$

$$X_{Fe} = 0.203 \quad [\equiv (X_{Mg}^0 + X_{Si}^0 + X_S^0 + X_{Ca}^0 + X_{Fe}^0)/X_{TOT}^0] ,$$

where

$$X_{TOT}^0 = X_C^0 + X_N^0 + X_O^0 + X_{Ne}^0 + X_{Mg}^0 + X_{Si}^0 + X_S^0 + X_{Ca}^0 + X_{Fe}^0 ,$$

and the superscript zero indicates the scaled solar abundances. By using such opacity tables, we have evolved, for the two quoted metallicities, three stellar models having masses $M = 0.6$, 0.8, and 1.0 $M_\odot$. The resulting evolutionary paths (*dashed lines*) are compared with the standard ones (*solid lines*) in Figures 16 and 17; it is evident that the two sets coincide extremely well, thus further confirming our findings. Only at $Z_0 = 10^{-3}$ do the two models of 1 $M_\odot$ present some differences, but, once again, such a mass lies outside the range of masses which is of interest for the GGC system.

3.2. *The* He-*burning Phase*

In the previous paragraph we discussed in detail the properties of the α-enhanced models in the evolutionary phases which extend from the MS up to the He flash. Here we will address the evolutionary phases which go from the central He-burning phases up to the clump luminosity on the asymptotic giant branch (AGB). In order to span the HB to some extent in color, we chose to follow the evolution of two models having masses equal to 0.6 and 0.70 $M_\odot$, for $Z_0 = 10^{-4}$, and of three models having masses equal to 0.55, 0.6, and 0.7 $M_\odot$ for $Z_0 = 10^{-3}$. For each of these five different cases we computed three evolutionary tracks: a standard one of metallicity Z_0, an α-enhanced one (with [α/Fe] = 0.6), and a standard one of metallicity $Z = 2.91Z_0$. This last track was obviously computed in order to verify whether also in these evolutionary phases the α-enhanced models coincide with the standard one having the same global metallicity. The values of the He core mass at the He flash and of the extra He were obtained by means of the relations reported in Paper II and are shown in Table 3 for the standard evolutionary tracks. Concerning the α-enhanced ones, since we have shown above that these two quantities are very well obtained by adopting the standard models having the same global metallicity, we used the same values adopted for the standard models having a metallicity $Z = 2.91Z_0$.

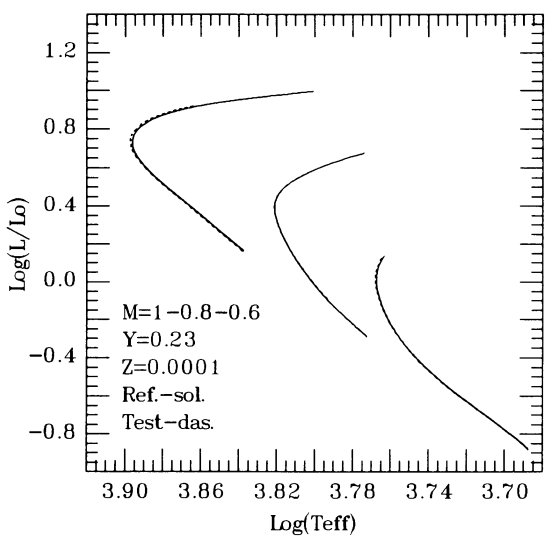

FIG. 16.—Comparison between standard scaled solar models (*solid lines*) having masses equal to 1, 0.8, and 0.6 $M_\odot$ ($Y = 0.23$ and $Z_0 = 10^{-4}$) and models obtained by adopting opacity tables computed by assuming a mixture formed by only O and Fe (*dashed lines*). See text for a wider discussion.

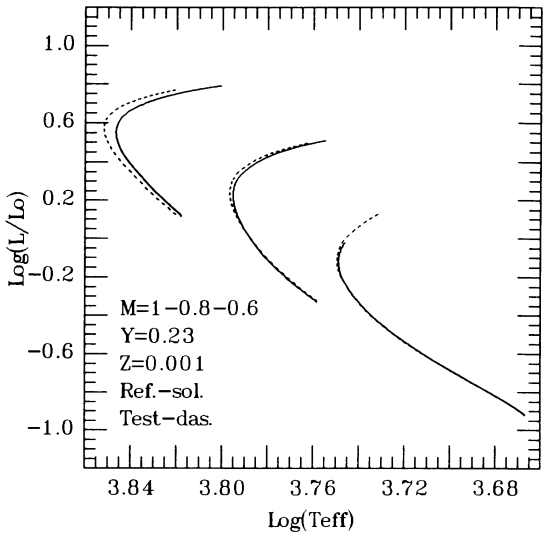

FIG. 17.—Same comparison as in Fig. 16, but for $Z_0 = 10^{-3}$

Figures 18 and 19 show, for the two quoted metallicities, the standard reference tracks (*dashed lines*), the α-enhanced ones (*dotted lines*), and the standard models having the same global metallicity as the α-enhanced ones (*solid lines*). Although the match between the α-enhanced and rescaled models is not as good as in previous evolutionary phases, nonetheless it is still possible to adopt the rescaled, instead of the enhanced, models without losing much accuracy. For the sake of clarity, in addition to the models discussed above we have computed other HB models in order to define the zero-age horizontal branch (ZAHB) accurately. Figure 20 shows, for $Z_0 = 10^{-4}$ (panel *a*) and for $Z_0 = 10^{-3}$ (panel *b*), the ZAHBs corresponding to the standard, rescaled, and enhanced cases, respectively, as dashed, solid and long-dashed lines. This figure shows quite clearly that the enhanced and rescaled ZAHBs are in very good agreement and, in particular, that the HB luminosity at the level of the RR Lyrae stars obtained by means of the rescaled models is almost coincident with that obtained by adopting the enhanced ones (the largest difference, in luminosity, between the rescaled and enhanced ZAHBs at $\log T_{eff} = 3.85$ being equal to $\Delta \log (L/L_\odot) \cong 0.0087$ at $Z_0 = 10^{-3}$). Actually, the effective temperatures also are, in general, in good agreement. The largest difference concerns the 0.6 $M_\odot$ $Z = 10^{-3}$ model: in

TABLE 3

VALUES OF He CORE MASS AND OF THE EXTRA He AT THE He FLASH

Z (1)	M_c (2)	δY (3)
10^{-4}	0.5037	0.008
10^{-3}	0.4932	0.013
2.91×10^{-4}	0.4988	0.010
2.91×10^{-3}	0.4883	0.017

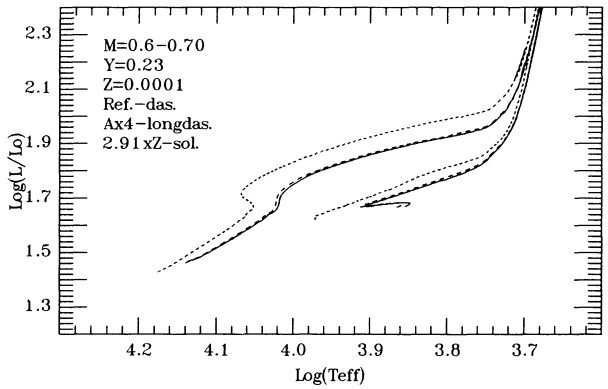

FIG. 18.—He-burning evolutionary tracks relative to the masses 0.6 and 0.7 $M_\odot$, $Y = 0.23$, and $Z_0 = 10^{-4}$: the dashed lines refer to the standard reference models, the dotted lines refer to the α-enhanced (by a factor of 4) models, while the solid lines refer to the standard models having $Z_0 = 2.91 \times 10^{-4}$.

this case the enhanced and rescaled models are shifted in temperature, with respect to each other, by $\Delta \log T_{\rm eff} \simeq 0.02$. The only practical consequence of such an effect is that the rescaled ZAHBs have masses slightly smaller (by less than 0.01 $M_\odot$) in the instability strip with respect to the ones which one would obtain by using the enhanced ZAHB. It is also worth noting that the clump on the AGB is perfectly simulated by the rescaled models.

We therefore conclude that for these evolutionary phases the α-enhanced models may be obtained again by adopting the standard scaled solar models having the same global metallicity.

4. DISCUSSION AND CONCLUSIONS

In the previous sections we have shown that, in spite of the fact that low-temperature α-enhanced opacities are still lacking, the α-enhanced models may be computed as a consequence of the fact that the metal contribution to such opacities does not influence the path of a stellar model from the MS up to beyond the TO, the key properties of the evolution all along the RGB phase, or the evolutionary properties in the following HB phase. The only feature which depends on the metal contribution to the low-temperature opacities is the location of the RGB: therefore, it totally depends on our (rather reasonable)

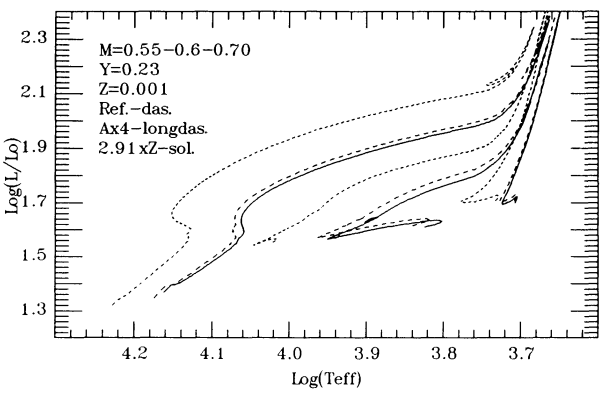

FIG. 19.—He-burning evolutionary tracks relative to the masses 0.55, 0.6, and 0.7 $M_\odot$, $Y = 0.23$, and $Z_0 = 10^{-3}$: the dashed lines refer to the standard reference models, the dotted lines refer to the α-enhanced (by a factor of 4) models while the solid lines refer to the standard models having $Z_0 = 2.91 \times 10^{-3}$.

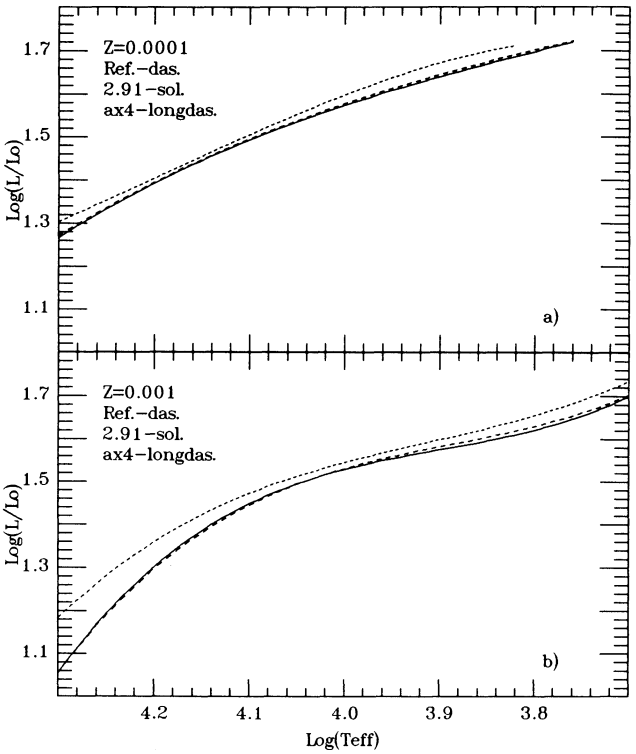

FIG. 20.—Comparison among different ZAHBs: the dashed, solid, and long-dashed lines refer, respectively, to the standard scaled solar metallicity Z_0, to the standard scaled solar metallicity having $Z = 2.91 Z_0$, and to the α-enhanced metallicity. (*a*) $Z_0 = 10^{-4}$; (*b*) $Z_0 = 10^{-3}$.

assumption that the α-elements behave similarly to Fe as electron donors at temperatures lower than 12,000 K.

Before proceeding further, let us comment on (*a*) the fact that in all the tests described above we used always the solar $T(\tau)$ relation as the outer boundary condition of the models instead of appropriate α-enhanced models of atmosphere, and (*b*) the calibration of the effective temperatures of the models.

With regard to the first point, let us remind the reader that (1) α-enhanced models of atmosphere are not available at present (and therefore cannot be used) and (2) even for the standard scaled solar models, the available models of atmosphere do not guarantee, at present, a reliability good enough to state that they represent a definitely better choice that the solar $T(\tau)$. Hence, in our opinion, the problem of the outer boundary conditions must be seen as one of the (well-known) factors of uncertainty which affect all the models produced up to now, and not the α-enhanced ones in particular: the present α-enhanced models constitute in any case the best approach to such a problem at the present time and a major improvement with respect to both the standard and O-enhanced (see below) stellar models.

With regard to the second point, the referee questioned the fact that our α-enhanced models require a proper recalibration of the mixing-length parameter as a consequence of the fact that they are not able to fit the "reliable" subdwarf Groombridge 1830. First, let us note that, as has been well known for a long time, the lower MS is not affected by the adopted value of the mixing-length parameter for the simple reason that the temperature gradient is only marginally superadiabatic in low-mass MS stars: Groombridge 1830 belongs to such a class of stars. Second, in our opinion the only reliable reference star

which may be used at present is the Sun: on the contrary, the use of another reference star, such as Groombridge 1830, in order to tune in a "refined way" the effective temperatures of the star models is highly hazardous. Just to mention a possible factor of uncertainty, it is well known that the metallicity of any star (included the quoted subdwarf) is not known with a precision better than, say, ± 0.2 dex (to the generous). Therefore, although the metallicity of this subdwarf is closer to that of the GGCs rather than to that of the Sun, it does not make any sense to consider such a star "more reliable" than the Sun. However, let us discuss the fit to Groombridge 1830 of our α-enhanced models. The main data concerning this star have been taken from Van Altena et al. (1988): they quote $[\mathrm{Fe/H}] \simeq -1.3$, $M_v = 6.79$, and $(B-V) = 0.75$. We have shown in Paper II that our standard isochrone having $Z = 10^{-3}$ (i.e., $[\mathrm{Fe/H}] \simeq -1.3$) has a $(B-V)$ color, at $M_v = 6.79$, equal to 0.76 mag and hence that it fits this star nicely. If we now assume that the α-elements are overabundant by a factor of 4 in this star, as is suggested by the bulk of Population II stars, we should adopt the isochrone having $Z = 2.91 \times 10^{-3}$ (which corresponds to $[\mathrm{Fe/H}] \simeq -1.3$, and $[\alpha/\mathrm{Fe}] \simeq 0.6$); in such a case we would obtain, at the absolute visual magnitude quoted for this star, a $(B-V)$ color equal to 0.81, i.e., a value much too red with respect to the one quoted for this "reliable" subdwarf. Such a conclusion cannot be avoided if one makes the "very reasonable" assumption that Groombridge 1830 behaves similarly to the bulk of Population II stars. Actually, the presently available data concerning the abundance of the α-elements in this star indicate that it is only slightly α-enhanced (if at all). In particular, Tomkin & Lambert (1980) find $[\mathrm{Fe/H}] \cong -1.36$, $[\mathrm{Mg/Fe}] \cong 0.11$ and $[\mathrm{Ca/Fe}] \cong 0.12$; Peterson (1981) quotes [Si/Fe] and $[\mathrm{Ca/Fe}] \cong 0.25$; Gratton and Sneden (1987) quote $[\mathrm{Fe/H}] \cong -1.15$, $[\mathrm{Mg/Fe}] \cong 0.08$, and $[\mathrm{Si/Fe}] \cong 0.29$; while Smith, Lambert, & Ruck (1992) give $[\mathrm{Fe/H}] \cong -1.3$, $[\mathrm{Mg/Fe}] \cong 0.3$, and $[\mathrm{Ca/Fe}] \cong 0.3$. All these data show that the α-elements in this specific star are, at most, only marginally enhanced with respect to iron (in spite of the star's relatively low Fe abundance) and that a fair *upper* limit to such an enhancement may be safely settled at 0.3 dex. By the way, such an occurrence constitutes the most striking confirmation that it is very hazardous, at present, to calibrate the theoretical models on a star other than the Sun. However, on the basis of the available observational data, the fit to Groombridge 1830 requires the adoption of isochrones having $[\alpha/\mathrm{Fe}] \simeq 0.3$ and not $[\alpha/\mathrm{Fe}] \simeq 0.6$ (the value suggested by the bulk of Population II stars). Hence, by adopting the isochrone having $Z = 1.64 \times 10^{-3}$ (which corresponds to $[\mathrm{Fe/H}] \simeq -1.3$ and $[\alpha/\mathrm{Fe}] = 0.3$), we get, at $M_v = 6.79$, a value $(B-V) = 0.78$ mag. Such a value is compatible with the one quoted for Groombridge 1830 because of the following facts: (1) the observed $(B-V)$ color of this star is uncertain by, at least, ± 0.01 mag; (2) the dependence of the $(B-V)$ color on the metallicity is rather strong around $Z = 10^{-3}$ [in particular, an uncertainty of ± 0.2 dex in the metallicity would imply a variation in the predicted $(B-V)$ color of ± 0.02 mag]; (3) the adoption of a log T_{eff}–$(B-V)$ relation more recent (Buser & Kurucz 1992) with respect to the one adopted in Paper II (VB85) would lead to a theoretical $(B-V)$ color (for Groombridge 1830) bluer by 0.03 mag (Salaris, Straniero, & Chieffi 1993); and (4) the models of atmosphere adopted by Smith et al. (1992) in order to determine the abundances of Ca and Mg in Groombridge 1830 predict a $(B-V)$ color of 0.8 mag (i.e., 0.05 mag redder than the observed value!), a value that they consider reasonably close to the observed one of 0.75 mag. Therefore, we conclude that our α-enhanced isochrones are compatible with the quoted subdwarf and that they must not be recalibrated.

Coming back to our discussion, we have shown that the α-enhanced models practically coincide with the standard scaled solar, properly rescaled, models if the condition

$$\left[\frac{X_{\mathrm{C}} + X_{\mathrm{N}} + X_{\mathrm{O}} + X_{\mathrm{Ne}}}{X_{\mathrm{Mg}} + X_{\mathrm{Si}} + X_{\mathrm{S}} + X_{\mathrm{Ca}} + X_{\mathrm{Fe}}}\right] \simeq 0 \qquad (1)$$

is satisfied. In such a case, denoting by f_α the average enhancement of the α-elements, the rescaling formula which relates the nonenhanced scaled solar metallicity Z_0 to the scaled solar one which mimics the α-enhancement, Z, may be written as

$$Z = Z_0(0.638 f_\alpha + 0.362) \qquad (2)$$

or, alternatively, as

$$[\mathrm{M/H}] \cong [\mathrm{Fe/H}] + \log(0.638 f_\alpha + 0.362)\,, \qquad (3)$$

where [M/H] denotes the global metallicity (this relation obviously gives $[\mathrm{M/H}] = [\mathrm{Fe/H}]$ for $f_\alpha = 1$).

Of course, if the condition expressed by equation (1) is not confirmed by future work, it follows that such a rescaling no longer holds. Let us underline the fact that the good equivalence between α-enhanced models and the standard ones having the same global metallicity depends only on condition (1) and not on the adopted value of the mixing-length parameter. For example, if in the future it is proved necessary to adopt a value of the mixing-length parameter of, say, 2.3, the α-enhanced models could still be obtained by means of relation (2) or relation (3), provided that the standard (i.e., scaled solar) isochrones were computed by adopting a value of the mixing-length parameter equal to 2.3.

The possibility of obtaining the α-enhanced isochrones by means of a simple rescaling of the standard scaled solar metallicity, although not expected a priori, has quite nice consequences. In fact, all the isochrones available in the literature (and not necessarily our isochrones) may be used as α-enhanced ones, provided that the metallicity is properly obtained by means of expression (2) or expression (3). Moreover, it is possible to explore a wide range of possible overabundances without the necessity of recomputing a large set of models, which would mean the investment of a considerable amount of time and money. For example, all the analytic fits of the quantities of interest that we presented in Paper II as a function of both the age and the metallicity remain valid provided, once again, that the metallicity to be used in the relations is properly determined.

An important consequence of the present work on the α-elements is that a ranking of the GGCs as a function only of [Fe/H] may be deeply misleading. In fact, we have shown that all the features of an isochrone depend significantly on all nine of the most abundant elements (C, N, O, Ne, Mg, Si, S, Ca, and Fe) and in particular on the global abundances of the two groups of elements (C + N + O + Ne) and (Mg + Si + S + Ca + Fe). Just to give a couple of examples, the parameter $(B-V)_{0,g}$ which is usually calibrated as a function of [Fe/H] should be calibrated, on the contrary, as a function of [(Mg + Si + S + Ca + Fe)/H], which are the elements which contribute to determine the slope of the RGB (let us remark that even in the scaled solar mixture the total abun-

dance of Mg + Si + S + Ca is larger than that of Fe). On the contrary, the "metallicity" which determines the location of the MS is [(C + N + O + Ne + Mg + Si + S + Ca + Fe)/H], i.e., the global metallicity [M/H], since all these elements influence its actual location in the H-R diagram. Another very important consequence of the present results is that, at variance with the TO region, since both the MS and the RGB locations are widely independent of the age, and since these two loci are not similarly influenced by the metallicity, it follows that, were it possible to match simultaneously both the MSs and the RGBs of two given GGCs by shifting the loci of one of them with respect to that of the other, then they must have roughly comparable global metallicities; if, after the shifting, the TOs coincide, it follows that they also have similar ages, while, if the TOs do not match, the two clusters must have different ages.

Let us now briefly discuss the O-enhanced models. Since the presently available observational data show that all the α-elements are overabundant with respect to iron, and since it is possible to compute α-enhanced models (see above), there is really no reason to compute such models. However, since O-enhanced models have been recently produced (e.g., VandenBerg 1992; Bergbusch & VandenBerg 1992) and used to fit the GGCs, we have computed a set of oxygen-enhanced isochrones (by a factor of 4) for the two metallicities $Z_0 = 10^{-4}$ and $Z_0 = 10^{-3}$ and ages between 10 and 20 Gyr in order to illustrate the differences between O- and α-enhanced isochrones. Figures 21 and 22 show, for the two quoted metallicities, two selected isochrones having, respectively, $t = 12$ and $t = 18$ Gyr. The solid, dotted, and dashed lines refer, respectively, to the standard, O- and α-enhanced isochrones. From both the figures it can be seen that the O-overabundance mainly alters the TO, while the MS is only slightly affected and the RGB untouched. The enhancement of all the α-elements leads, on the contrary, to isochrones significantly different with respect to the standard ones, since they affect all the evolutionary phases. In particular, they are redder with respect to both the standard and the O-enhanced isochrones and have a TO luminosity even dimmer than that obtained by enhancing only the oxygen. In order to quantify the differences among these three sets of isochrones, we show in Figure 23 the visual magnitude of the TO as a function of the age for the two metallicities; the solid, long-dashed, and dashed lines refer, respectively, to the standard, O- and α-enhanced cases. The O- and α-enhanced isochrones imply an age reduction of, respectively, ~0.7 and 1 Gyr (at $Z_0 = 10^{-4}$) and of 1 Gyr and 1.5 Gyr (at $Z_0 = 10^{-3}$) per 0.3 dex in the overabundance of the α-elements. Concerning the slope of the $(B-V)$ color of the MS (at $M_v = 6$) as a function of the metallicity, we obtain, for the O-enhanced isochrones,

$$\frac{\Delta(B-V)_{\rm MS}}{\Delta \log Z} = 0.074 \quad \text{(O-enhanced case)},$$

a value which must be compared with those obtained for the standard and α-enhanced cases (given in the previous section). In particular, the enhancement by a factor of 4 of only oxygen underestimates the scaling of the MS as a function of the metallicity with respect to the scaling obtained by enhancing all the α-elements. By the way, note that such a relation is quite important, since, e.g., it is the main ingredient of one of the methods which are used in order to determine the relative distances of the GGCs, namely, the MS fitting method

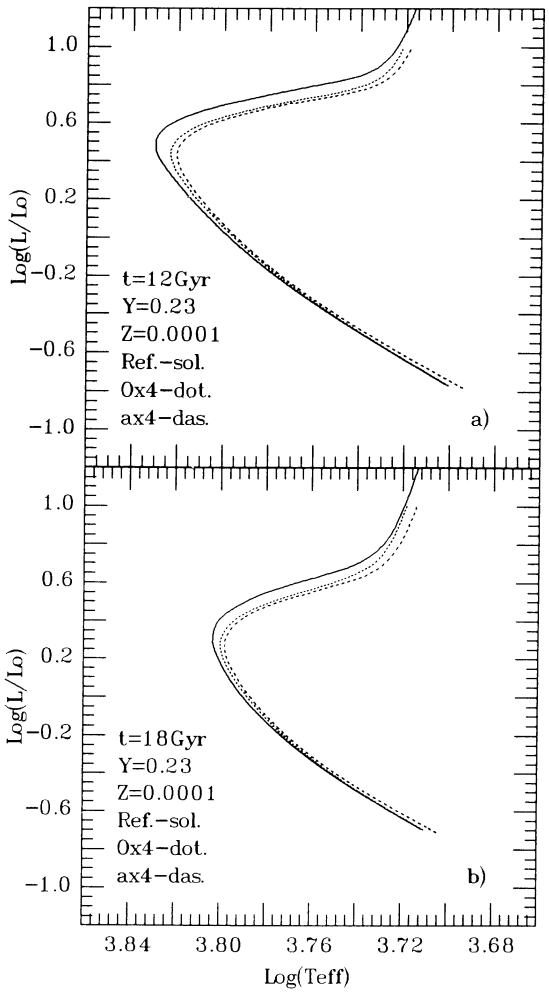

FIG. 21.—Comparison among standard (*solid line*), O-enhanced (*dotted line*), and α-enhanced (*dashed line*) isochrones having $Z_0 = 10^{-4}$, for the two ages (*a*) 12 and (*b*) 18 Gyr.

(Buonanno, Corsi, & Fusi Pecci 1989; Sandage & Cacciari 1990; Carney, Strom, & Jones 1992). Another crucial point concerns the $(B-V)$ color difference between the TO and the base of the RGB. In Paper II we have shown that such a quantity depends strongly on the age and mildly on the metallicity, and therefore it may be used as a strong age indicator. Such a color difference has been used by us in Paper II in order to derive the ages of a selected group of GGCs (we will turn to this subject below). In a recent paper VandenBerg & Stetson (1991), by adopting O-enhanced isochrones, showed that the $(B-V)$ color difference between the TO and the base of the RGB depends on the possible oxygen overabundance, and they gave a relation linking the age of a cluster to the adopted O-overabundance. Such a result obviously depends on the fact that, by neglecting the contribution of the other α-elements, only the $(B-V)$ color of the TO is altered with respect to the standard case, while the RGB color remains unaffected. On the contrary, since the inclusion of the enhancement of all the α-elements affects the colors both at the TO and at the base of the RGB and shifts them in the same direction (lowers the effective temperatures), $\Delta(B-V)$ is not significantly affected by the enhancement. In particular, since the α-enhancement mimics a larger scaled solar metallicity, and since the standard

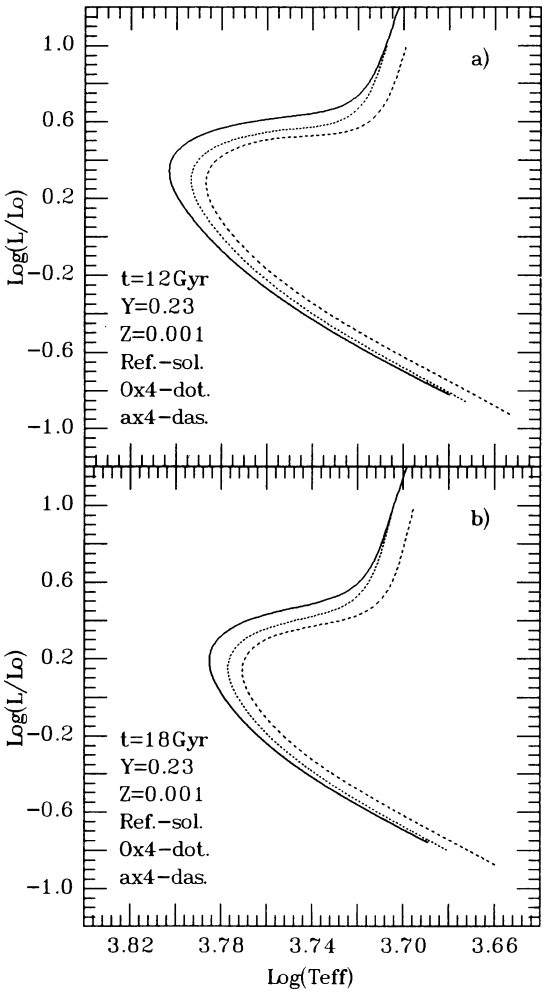

FIG. 22.—Same comparison as in Fig. 21, but for $Z_0 = 10^{-3}$

scaled solar isochrones show that $\Delta(B-V)$ only mildly depends on the metallicity, it follows that, at variance with the results obtained by enhancing only the oxygen, the ages (absolute and/or relative) derived by means of $\Delta(B-V)$ are not affected by the possible enhancement of the α-elements. Hence, from all this discussion, we conclude that the proper inclusion of the α-elements cannot be neglected in the computation of isochrones to be used to fit the GGCs.

Let us check, at this point, how, and to what extent, the fits to the GGCs obtained by adopting the standard isochrones are modified by adopting the α-enhanced ones. In particular, let us consider the problem of the determination of the ages of the GGCs by adopting two different methods: the ΔV(HB − TO) method, which uses the M_v difference between the TO and the HB at the level of the RR Lyrae stars, and the $\Delta(B-V)$ method, which uses the $(B-V)$ color difference between the TO and the base of the RGB. First, let us remind the reader that both methods are independent of the distance modulus and the reddening. Before discussing the results obtained by applying these two methods, let us briefly comment on their reliability. In all cases in which one wants to compare a theoretical prediction with an observable quantity, it is important that both are as reliable as possible. Unfortunately, neither of the two methods presents a comparable reliability of the two quoted quantities.

Concerning the ΔV(HB − TO) method, it can be said that its theoretical predictability is widely considered relatively good, since it makes use only of the theoretical luminosities and not of the radii (or, equivalently, of the effective temperatures). The situation from the observation point of view is much worse, since (1) a consistent fraction of clusters do not present at all an HB populated in the region of the RR Lyrae stars; (2) the luminosity around the TO region is almost vertical (which means that it is not so easy to fix the luminosity of the bluest point); and (3) the visual magnitudes of the HB at the level of the RR Lyrae stars, and of the TO, for a given cluster, are often derived by collecting results obtained by different authors with very different detectors. In particular, most of the determinations of the HB luminosities still rely on photographic photometries, while the TO luminosities are obtained by means of CCD data.

It follows that, for most of the clusters, a conservative average estimate of the error to be associated with the determination of ΔV is of the order of ± 0.15 mag. Since the derivative of the age with respect to ΔV is $\cong 17$ Gyr mag^{-1}, it is evident that such a determination of the age of a cluster presents an

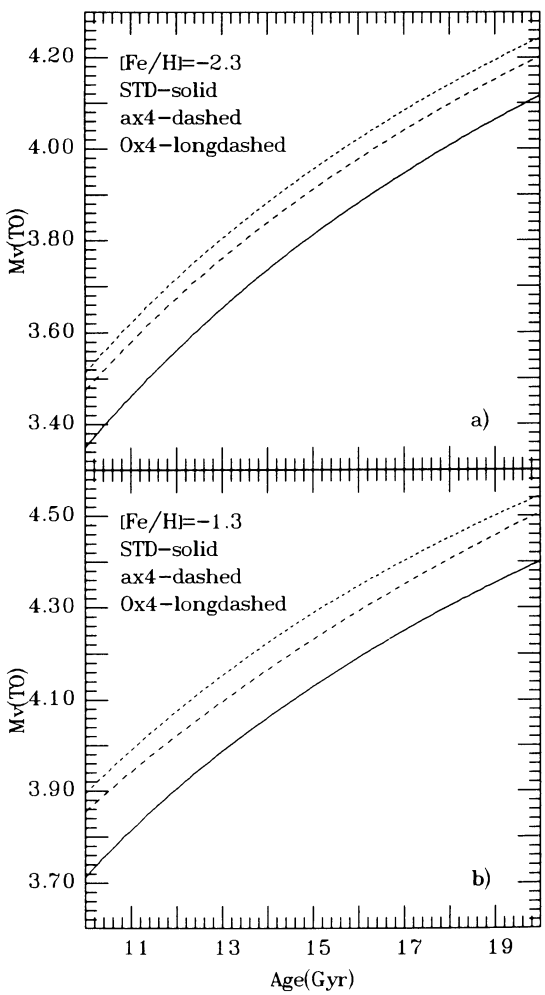

FIG. 23.—Plot of the visual magnitude of the TO vs. age: the solid line refers to the standard scaled solar case, the dashed line refers to the case in which the α-elements are enhanced by a factor of 4, while the long-dashed line refers to the case in which O is enhanced by a factor of 4. (*a*) $Z_0 = 10^{-4}$; (*b*) $Z_0 = 10^{-3}$.

internal error of ± 2.5 Gyr. Therefore, two or more clusters whose ΔV values are "equal" within the error bars may be considered either coeval or as having an age spread of several gigayears. Moreover, there is often the habit of adopting an average ΔV for all the clusters, *since they are rather similar*. It is worth noting that by neglecting such *small* differences one practically *cancels out* a priori a possible age spread of 4–5 Gyr or more.

The opposite occurs in the case of the $\Delta(B-V)$ method, since in this case the theoretical predictions are less precise than the observed data. In fact, the theoretical determination of the radius (or, alternatively, of the effective temperature) and, in turn, of the $(B-V)$ color is in general considered not reliable owing to our still poor treatment of, e.g., the low-temperature opacities, the superadiabatic convective mechanisms, and the $\log T_{\rm eff}$–$(B-V)$ relation. Nonetheless, since this method requires the determination of just the $(B-V)$ color difference between the TO and the base of the RGB, it is hoped that this quantity is less uncertain that is the $(B-V)$ color itself. For example, the adoption of the $\log T_{\rm eff}$–$(B-V)$ relation given by Buser & Kurucz (1992) leads to isochrones which are significantly bluer than those obtained by adopting the analogous relation given by VB85, but to the $\Delta(B-V)$ fairly similar to that obtained by adopting the VB85 relation (Salaris et al. 1993). Moreover, in order to check the reliability of the temperatures of our models, we analyzed, in Paper II, both the small sample of available field subdwarfs (see above) and the ranking of the effective temperature of the RGB, at a given magnitude, versus [Fe/H] for a rather large sample of clusters (Frogel, Cohen, & Persson 1983). In both cases we found that our theoretical models led to a reasonably good fit to the data without the requirement of any changing of the mixing-length parameter α (which is fixed, as usual, by the Sun; see Paper I). In addition to that, a point in favor of this method is that it does not require a precise knowledge, a priori, of the metallicity of the clusters to be fitted. From the observational point of view $\Delta(B-V)$ is a quantity which may be quite well determined, since (1) the MS, the TO, and the base of the RGB of all the clusters are well populated, and (2) $\Delta(B-V)$ is almost independent of the adopted photometry. While point 1 does not deserve any comment, let us shortly comment on point 2. We have shown in Paper II four clusters for which photometry is available from more than one source; it is interesting to note that, in all four cases, although the different loci do not superpose, nonetheless they present very similar values of $\Delta(B-V)$. In other words, it appears that, at least in the four cases examined, fiducials obtained by different authors tend to have similar shapes.

From this short discussion concerning the reliability of these two methods in order to determine the ages of the GGCs, we feel confident in concluding that the two have comparable advantages as well as comparable disadvantages, and hence there is really no scientific reason to prefer one method over the other.

The use of the ΔV(HB − TO) method requires both a relation giving the TO visual magnitude as a function of the age and of metallicity and another giving the visual magnitude of the HB at the level of the RR Lyrae stars as a function of the metallicity. The first relation has already been reported in Paper II, while the second may be derived from the HB models computed by Castellani, Chieffi, & Pulone (1991, hereafter CCP19) (with the same code adopted in Paper II and in the present paper), and may be expressed as

$$M_v(\mathrm{RR}) = 1.1595 + 0.5047[\mathrm{M/H}] + 0.086[\mathrm{M/H}]^2 \,. \quad (4)$$

By combining this relation with the one which gives M_v(TO) as a function of the age and the metallicity (Paper II),

$$M_v(\mathrm{TO}) = 1.4496 + 3.4388 \log t_9 - 0.6503\,[\log (t_9)]^2 + 0.6919[\mathrm{M/H}] + 0.0171[\mathrm{M/H}]^2 - (0.2657 \log t_9[\mathrm{M/H}) \,, \quad (5)$$

one may obtain the ΔV for each chosen age and metallicity. By interpolating within a large grid of Δ values obtained in such a way for different ages and metallicities, it is possible to derive the formula

$$\log t_9 = -0.2506 + 0.4155\,\Delta V + 0.0508[\mathrm{M/H}] + 0.0286[\mathrm{M/H}]^2 \,, \quad (6)$$

where t_9 indicates the age in Gyr and [M/H] the global metallicity. By means of relations (6) and (2) (or relation [3]) we can derive the age of a cluster once ΔV, [Fe/H], and the average enhancing factor f_α of the α-elements are known. The first thing which is interesting to note is that relation (6) shows a quite mild dependence on the metallicity in the range of interest for the GGCs. In fact, it is almost flat in the region $-1.5 < [\mathrm{M/H}] < -0.5$, while it shows a mild dependence at the lowest metallicities. In particular, the strongest dependence occurs at the low-metallicity end ($[\mathrm{M/H}] \simeq -2.3$) where the age varies by $\simeq 1$ Gyr per 0.3 dex of increase of the metallicity. Since the enhancement of the α-elements may be interpreted as a simple increase of the metallicity, the very important result follows that the ages of the GGCs derived by such a method are not strongly affected by a reasonable enhancement of the α-elements. Since CSD92 addressed the same problem we are facing, i.e., the analysis of the ΔV values of a sample of clusters by adopting a new set of α-enhanced isochrones computed by them, we decided to use their sample of 33 clusters and the ΔV values reported in their Table 3. Our Table 4 reports the names of the clusters in column (1), the ΔV values as given by CSD92 in column (2), and the [Fe/H] values as given by Zinn & West (1984, hereafter ZW84), in column (3). Columns (4) and (5) show, respectively, the ages (in Gyr) which are obtained, respectively, for the standard and enhanced ($[\alpha/\mathrm{Fe}] = 0.6$) cases. It is evident that, as we have already noted above, an enhancement of the α-elements by a factor of 4 does not alter significantly either the absolute ages or the age spread of this sample of GGCs. In fact, the very metal-poor clusters, which present the largest age reduction, are $\simeq 1.3$ Gyr younger than in the standard case, while the clusters of higher metallicity are progressively much less influenced by the α-enhancement. Of course the adoption of a smaller enhancement factor would lead to even smaller differences with respect to the standard case. Figure 24 shows, for the enhanced case, the ages derived by means of the ΔV method (col. [5] in Table 4) as a function of [Fe/H] (col. [3] in Table 4). The first impression one has from this figure is a trend of the age with metallicity in the sense that the larger the metallicity, the younger the age. However, the ages of most of these clusters are confined between 14 and 18 Gyr, and since the average error bar associated with each of these age determinations is of the order of ± 2.5 Gyr, it is clear that these data are perfectly compatible also with a picture in which most (not all) of the GGCs are coeval.

One could question, at this point, whether it is very safe to compare the ages derived for clusters having different metallicities for a number of reasons: for example, (*a*) the efficiency

TABLE 4

BASIC DATA FOR THE SAMPLE OF GALACTIC GLOBULAR CLUSTERS ANALYZED AND SUMMARY OF THE RESULTS OBTAINED

Name (1)	ΔV (2)	$[Fe/H]_{ZW84}$ (3)	$(t_9-\Delta V)_{std}$ (4)	$(t_9-\Delta V)_{enh}$ (5)	$[M/H]_{SC91}$ (6)	$t_9-\Delta(B-V)$ (7)
NGC 104 (47 Tuc)	3.65	−0.71	17.6	18.0	−0.63	12
NGC 288	3.60	−1.40	17.0	16.7	−1.68	19
NGC 362	3.42	−1.27	14.2	14.1	−1.29	14
NGC 1261	3.57	−1.31	16.4	16.2	...	...
NGC 1851	3.34	−1.36	13.2	13.0	...	...
NGC 1094 (M79)	3.40	−1.69	14.4	13.9	...	...
NGC 2298	3.49	−1.85	16.0	15.3	...	...
NGC 2808	3.50	−1.37	15.4	15.2	...	...
NGC 3201	3.44	−1.61	14.8	14.4	...	...
NGC 4147	3.60	−1.80	17.6	16.9	...	...
Ruprecht 106	3.15	−1.69	11.3	10.9	−2.04	18
NGC 4590 (M68)	3.39	−2.09	15.0	14.2	−2.04	19
NGC 5053	3.50	−2.41	17.7	16.3	...	...
NGC 5272 (M3)	3.52	−1.66	16.1	15.6	−1.29	18
NGC 5466	3.58	−2.22	18.4	17.2	...	...
Pal 5	3.40	−1.47	14.1	13.8	...	...
NGC 5897	3.60	−1.68	17.4	16.8	...	...
NGC 5904 (M5)	3.49	−1.40	15.3	15.0	−1.21	16
NGC 6101	3.40	−1.81	14.6	14.0	−1.82	20
NGC 6121 (M4)	3.55	−1.33	16.7	16.8	...	...
NGC 6171 (M107)	3.60	−0.99	16.1	15.9	−1.30	19
NGC 6205 (M13)	3.55	−1.65	16.5	16.0	...	...
NGC 6341 (M92)	3.65	−2.24	19.8	18.4	−2.44	19
NGC 6397	3.64	−1.91	18.6	17.7	...	...
NGC 6752	3.65	−1.54	18.0	17.6	−1.62	16
NGC 6809 (M55)	3.55	−1.82	16.9	16.1	...	...
NGC 7006	3.55	−1.59	16.4	16.0	...	...
NGC 7078 (M15)	3.54	−2.15	17.5	16.4	...	...
NGC 7099 (M30)	3.53	−2.13	17.3	16.2	−2.14	20
Pal 12	3.30	−1.14	12.6	12.6	−0.92	11
Pal 13	3.39	−1.79	14.4	13.8	...	...
NGC 7492	3.61	−1.82	17.8	17.1	−1.82	20

of the convection (which means a variation of the mixing-length parameter within the classical scheme of description of the convection), (*b*) the opacity, (*c*) the He core mass at the He flash, (*d*) the extra He brought to the surface as a consequence of the first dredge-up, and so on, may depend differently and more substantially on the metallicity than the presently available theoretical prescriptions. Therefore, clusters having different metallicities may appear coeval or not, simply as a consequence of an incorrect knowledge of the scaling of one (or more) of these quantities with respect to the metallicity. On such a basis one could therefore question the reliability of a (possible) trend of age with metallicity. However, the data reported in Figure 24 show that, *at each metallicity*, an age spread of, say, 4 Gyr is present. Although we have already pointed out that the error bar is quite large, the existence of such a systematic result weakly tends to favor a scenario in which the GGCs are not coeval.

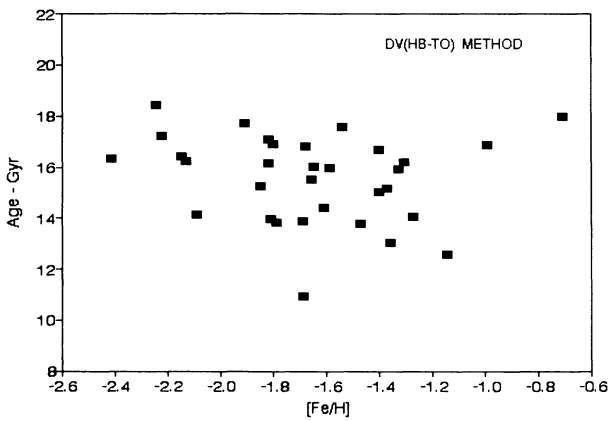

FIG. 24.—Plot of the ages obtained for a sample of Galactic globular clusters (listed in Table 4) by means of the ΔV(HB − TO) method vs. the metallicity quoted by Zinn & West (1984).

Let us note, at this point, that the ages derived by CSD92 present a similar spread but are systematically smaller by $\cong 2$ Gyr at low and intermediate metallicities and by $\cong 3$ Gyr at [Fe/H] $\cong 0.6$. This is probably due to the following facts:

1. The relation $M_v(RR) = f([Fe/H])$ obtained by CCP91 is different from the one presented by Lee (1990); in fact, while Lee uses synthetic HBs in order to derive the luminosity at the level of the RR Lyrae stars, CCP91 use the ZAHBs; and while Lee adopts a linear dependence of the HB luminosity versus the metallicity, CCP91 adopt a parabolic fit, which better reproduces their theoretical HBs. Figure 25 shows the two relations. It is evident that there is essentially a zero-point difference of the order of $\simeq 0.05$ mag between the two relations at the low and intermediate metallicities, while the difference grows at the larger ones (up to 0.2 mag at [Fe/H] = −0.6). The differences mentioned above may explain roughly half of the existing difference between the ages obtained in the present work and those obtained by CSD92 at the low and intermediate metallicities, while it accounts for roughly 70% of the discrepancy at the higher metallicities.

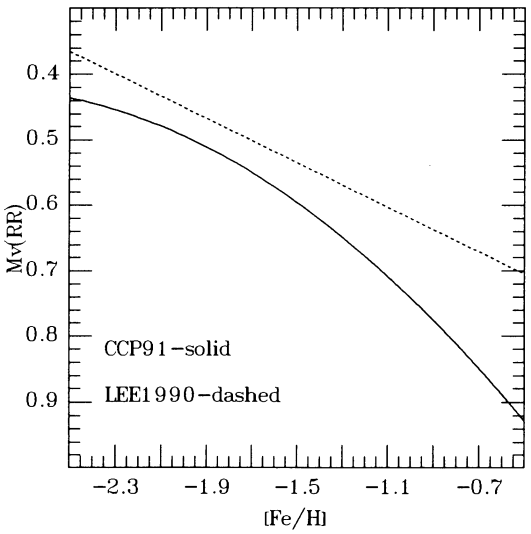

FIG. 25.—Plot of the HB visual magnitude at the level of the RR Lyrae stars vs. metallicity: the solid line represents the relation obtained by Castellani, Chieffi, & Pulone (1991), while the dashed line represents that provided by Lee (1990).

2. The Lee relation adopted by CSD92 is scaled solar and not α-enhanced. We have shown above that the inclusion of α-enhancement in the computation of the HB models alters the HB luminosity and therefore cannot be neglected. Note also that the α-enhanced HB models computed by Bencivenni et al. (1991) agree with the present ones.

Let us now turn to the $\Delta(B-V)$ method. The strength of this method actually relies on the theoretical prediction that the color difference between the TO and the base of the RGB is almost unaffected by the metallicity, and it therefore follows that the ages derived by adopting this method are also insensitive to the overabundance of the α-elements. Therefore, the ages derived in Paper II for the same of GGCs analyzed in that paper may still be considered valid in the case of an enhancement of the α-elements. The metallicities and the ages obtained in Paper II are reported in columns (6) and (7) of Table 4 for the 10 clusters in common between the two samples. In order to increase the sample of clusters for which an age determination was available by means of the $\Delta(B-V)$ method, we analyzed also the clusters Ruprecht 106 (Buonanno et al. 1990), NGC 6101 (Sarajedini & Da Costa 1991), NGC 7492 (Cote, Richer, & Fahlman 1991) and M107 (Ferraro & Piotto 1992) by adopting the same technique used in Paper II. The resulting metallicities and ages are also reported in columns (6) and (7) of Table 4. The ages obtained by the $\Delta(B-V)$ method, plotted against the metallicity, are shown in Figure 26. Note that the metallicities on the abscissa are the ones obtained by using our method and may be safely considered as global metallicities (see Paper II), i.e., they already include the possible overabundance of the α-elements. It is quite evident that a relation seems to exist between the age and the global metallicity. Although the formal error is in this case much smaller than that obtained for the ΔV method, the suspicion that the present determination of the radii is not very reliable leaves room also for a coevality of the GGCs. The warnings already discussed for the ΔV method, concerning the reliability of ages derived for clusters having different metallicities, obviously applies also to this method, and therefore one could question again the reliability of the trend of age with metallicity which appears in Figure 26. It is worth noting, however, that the adoption of this method greatly reduces the scatter of the ages at each fixed metallicity; it is only at the intermediate ones that a probably meaningful scatter still persists.

The reader may suspect that, while the ages determined by adopting the $\Delta(B-V)$ method are practically unaffected by the overabundance of the α-elements, the distance moduli derived for each cluster could be a function of such an overabundance. Actually this is not the case. If fact, the method we have proposed in Paper II in order to fit the GGCs is a two-step method: once the age has been determined by fitting the color difference between the TO and the base of the RGB, two out of the other three quantities—reddening, distance modulus, and metallicity—may be expressed as function of the third one, and we have chosen the reddening to be the independent variable. Therefore, both the metallicity and the distance modulus are unequivocally determined once a value for the reddening has been chosen. Note that such a derived metallicity is a global metallicity, and therefore it already includes the possible overabundance of the α-elements. This means that within our scheme it does not make any sense to try to derive a relation between the chosen metallicity and the distance modulus, for the simple reason that both are *results of the fitting* and are not input parameters. As a last comment, let us underline the fact that the distance moduli we obtain by using our two-step method are in very good agreement with the ones available in the literature, and since such a topic is in depth discussed in Paper II, we refer the reader to such a paper for a wider discussion.

Having discussed separately the results obtained by adopting the two quoted methods, it is of great interest to compare the two sets of results. Figure 27 shows the plot of the ages obtained by means of the ΔV method versus the ones obtained by adopting the $\Delta(B-V)$ method. The solid line shows the locus which corresponds to the same determination of the age, while the two dotted lines make evident the "compatibility strip," which corresponds to the age variation by ± 3.5 Gyr (i.e., the sum of the average error bars to be associated with each of the two methods). The first thing to note is that most of the clusters lie within such a "compatibility strip," and therefore one can formally say that the two methods are essentially compatible. Actually such a strip is so large that one should

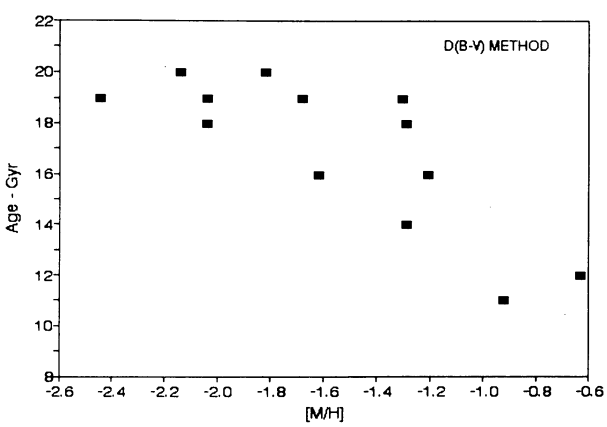

FIG. 26.—Plot of the ages obtained for a sample of Galactic globular clusters (listed in Table 4) by means of the $\Delta(B-V)$ method vs. the metallicity quoted by Straniero & Chieffi (1991).

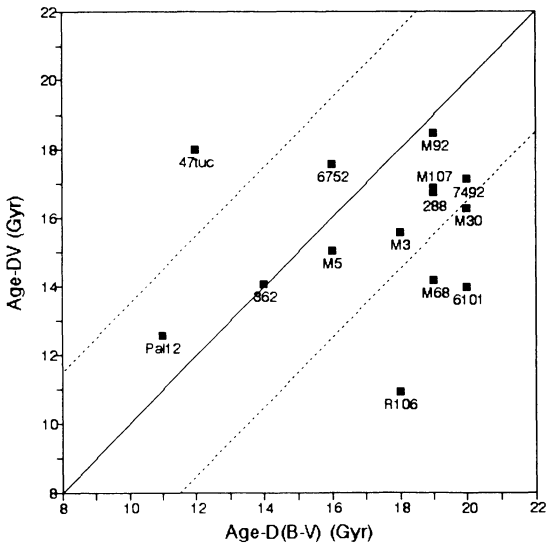

FIG. 27.—Plot of the ages obtained for a sample of Galactic globular clusters (listed in Table 4) by means of the ΔV(HB − TO method vs. those obtained by using the $\Delta(B-V)$ method. The dotted lines identify a strip of compatibility. See text for more details.

honestly say that it is not presently possible to establish whether the two methods give similar ages (within, say, ± 1 Gyr) or not. However, even though this "compatibility strip" is so large, four out of the 14 clusters remain outside this marginal compatibility. Let us finally briefly comment on the four outlying points.

The Galactic globular clusters 47 Tucanae, which shows a large discrepancy between the ages derived by means of the two methods, shows a ΔV which closely resembles that of M92 (a typical very metal-poor cluster) while the $\Delta(B-V)$ turns out to be very similar to that of clusters of relatively similar metallicity (Pal 12 and NGC 362). Such an occurrence cannot be easily explained by a wrong calibration of $\Delta(B-V)$ versus age, since, if we assume that the point corresponding to 47 Tuc must be shifted horizontally up to an age of 18 Gyr, the other metal-rich clusters, and in particular Pal 12, which has a similar $\Delta(B-V)$ and a not very different metallicity, should also be shifted horizontally toward much larger ages and would fall, in this case, at the right side of the strip, constituting once again an example of a contradictory situation in which the ages determined by means of the two methods give very different results. One could question the reliability of the HB luminosity obtained for such a cluster: since it has a very red HB, a severe mistake in determining the HB luminosity at the level of the RR Lyrae stars is possible. However, Pal, 12 also present a similarly red HB, but the ages derived by adopting the two different methods lead to very similar results.

The case of M68, NGC 6101, and Ruprecht 106, three metal-poor clusters, is even more intriguing. By shifting the fiducial of each of these clusters with respect to that of any of the other metal-poor clusters in the sample, it is possible to match both the MSs and the RGBs simultaneously. Since we have shown in the previous sections that the positions of the MS and of the RGB depend on the global metallicity, it follows that the simultaneous match of these features implies that the global metallicities of these clusters must be quite similar (within a factor of, say, 2). The additional observation that, once the MSs and the RGBs are simultaneously matched, the TOs are also close to each other constrains the possible age spread, within such a metal-poor group of GGCs, to within, say, 2 Gyr. Now, leaving aside the absolute values of the ages obtained by adopting the two methods, it is worth noting that while the $\Delta(B-V)$ method follows such an expectation (i.e., that these clusters have similar ages), the ΔV method gives an age spread of several gigayears. In our opinion such an occurrence is connected in some way to the HB luminosity rather than to the TO luminosity. The most trivial possibility is a wrong determination of the HB luminosity: for example, we note first that Carney et al. (1992) reanalyzed M92 and M68 and found that, contrary to previous estimates, these two have very similar ΔV values, and, second, we remark that evolutionary effects may mask the real location of the ZAHB. If this were not the case, one should explore why clusters of similar metallicities and ages have intrinsically different HB luminosities (slightly different initial He abundances? and why?).

As a final remark, we are expected to say whether the present results favor an age spread or the coevality for the GGCs system. The answer to this question is, in our opinion, so subjective that it resembles the old question whether a defendant is innocent until proved guilty or guilty until proved innocent (it goes without saying that for us the present data indicate that "innocence" means age spread). We leave such a decision to the reader.

It is a pleasure to thank Roberto Buonanno, Carlo Corsi, Marco Limongi, Alvio Renzini, & Amedeo Tornambè for many helpful discussions on the subject. Special thanks are due Roberto Buonanno and Carlo Corsi for providing their data concerning Ruprecht 106 and other clusters in a computer-readable format and for many long-lasting discussions concerning the ages of the Galactic globular clusters. Very special thanks go to Amedeo Tornambè for having forcefully pointed out to us, at the beginning of this work, that the α-elements other than oxygen are an important ingredient to be included in the model cooking.

REFERENCES

Abia, C., & Rebolo, R. 1989, ApJ, 347, 186
Anders, E., & Grevesse, N. 1989, Geochim. Cosmochim. Acta, 53, 197
Barbuy, B. 1988, A&A, 191, 121
Barbuy, B., Spite, F., & Spite M. 1985, A&A, 144, 343
Bazzano, A., Caputo, F., Sestili, M., & Castellani, V. 1982, A&A, 111, 312
Bencivenni, D., Caputo, F., Manteiga, M., & Quarta, M. L. 1991, ApJ, 380, 484
Bencivenni, D., Castellani, V., Tornambè, A., & Weiss, A. 1989, ApJ, 71, 109
Bergbusch, P. A., & VandenBerg, D. A. 1992, ApJS, 81, 163
Bessell, M. S., Sutherland, R. S., & Ruan, K. 1991, ApJ, 383, L71
Buonanno, R., Buscema, G., Fusi Pecci, F., Richer, H. B., & Fahlman, G. G. 1990, AJ, 100, 1811
Buonanno, R., Corsi, C. E., & Fusi Pecci, F. 1989, A&A, 216, 80
Buser, R., & Kurucz, R. L. 1992, A&A, 264, 557
Carney, B. W., Strom, J., & Jones, R. V. 1992, ApJ, 386, 663
Castellani, V., Chieffi, A., & Pulone, L. 1991, ApJS, 76, 911 (CCP91)
Castellani, V., & Tornambe, A. 1977, A&A, 61, 427
Chaboyer, B., Sarajedini, A., & Demarque, P. 1992, ApJ, 394, 515 (CSD92)
Chieffi, A., & Straniero, O. 1989, ApJS, 71, 47 (Paper I)
Chieffi, A., Straniero, O., & Salaris, M. 1991, in ASP Conf. Series, Vol. 13, The Formation and Evolution of Star Clusters, ed. K. Janes (San Francisco: ASP), 219
Clegg, R. E. S., Lembert, D. L., & Tomkin, J. 1981, ApJ, 250, 262
Cohen, J. G. 1978, ApJ, 223, 487
Cote, P., Richer, H. B., & Fahlman, G. G. 1991, AJ, 102, 1356
Cox, A. N., & Stewart, J. N. 1970a, ApJS, 19, 243
———. 1970b, ApJS, 19, 261
Cox, A. N., & Tabor, J. E. 1976, ApJS, 31, 271
Fahlman, G. G., Richer, H. B., & VandenBerg, D. A. 1985, ApJS, 58, 225

Ferraro, F. R., & Piotto, G. 1992, MNRAS, 255, 71
François, P. 1986a, A&A, 160, 264
———. 1986b, A&A, 165, 183
Frogel, J. A., & Persson, S. A. 1983, ApJ, 275, 773
Gratton, R. G. 1987, A&A, 177, 177
Gratton, R. G., & Ortolani, S. 1986, A&A, 169, 201
———. 1989, A&A, 211, 41
Gratton R. G., Quarta, M. L., & Ortolani, S. 1986, A&A, 169, 208
Gratton, R. G., & Sneden, C. 1987, A&A, 178, 179
Green, E. M., Demarque, P., & King, C. R. 1987, The Revised Yale Isochrones and Luminosity Functions (New Haven: Yale Univ).
Grevesse, N. 1984, Phys. Scripta, 78, 49
Hartwick, F. D. A., & VandenBerg, D. A. 1973, PASP, 85, 355
Hesser, J. E., Harris, W. E., VandenBerg, D. A., Allwright, J. W. B., Shot, P., & Stetson, P. B. 1987, PASP, 99, 739
Huebner, W. F., Merts, A. L., Magee Jr., N. H., & Argo, M. F. 1977, Los Alamos Sci. Lab. Rep., LA-6760-M
Iben, I., Jr. 1965, ApJ, 141, 993
Laird, J. B. 1986, ApJ, 303, 718
Lambert, D. L. 1989, in Cosmic Abundances of Matter, ed. C. J. Waddington (New York: AIP), 168
Lee, Y. W. 1990, ApJ, 363, 159
Leep, E. M., & Wallerstein, G. 1981, MNRAS, 196, 543
Luck, E. L., & Bond, H. E. 1981, ApJ, 244, 919
———. 1985, ApJ, 292, 559
Magain, P. 1985, A&A, 146, 95
———. 1987, A&A, 179, 176
———. 1989, A&A, 209, 211
Matteucci, F., & Greggio, L. 1986, A&A, 154, 279
Meyer, J. P. 1985, ApJS, 57, 173
Peterson, R. C. 1981, ApJ, 244, 289
Peterson, R. C., Kurucz, R. L., & Carney, B. W. 1990, ApJ, 350, 173
Pilachowski, C. A., Sneden, C., & Wallerstein, G. 1983, ApJS, 52, 241
Pilachowski, C. A., Wallerstein, G., & Leep, E. M. 1980, ApJ, 236, 508
Renzini, A. 1977, in Advanced Stages in Stellar Evolution, ed. P. Bouvier & A. Maeder (Geneva: Geneva Obs.), 151
Rood, R. T. 1981, in Physical Processes in Red Giants, ed. I. Iben Jr., & A. Renzini (Dordrecht: Reidel), 51
Ross, J. E., & Aller, L. H. 1976, Science 1991, 1223
Salaris, M., Straniero, O., & Chieffi, A. 1993, in preparation
Sandage, A., & Cacciari, C. 1990, ApJ, 350, 645
Sarajedini, A., & Da Costa, G. S. 1991, AJ, 102, 628
Simoda, M., & Iben, I., Jr. 1968, ApJ, 152, 509
———. 1970, ApJS, 183, 81
Smith, G., Lambert, D. L., & Ruck, M. J. 1992, A&A, 263, 249
Sneden, C., Lambert, D. L., & Whitaker, R. W. 1979, ApJ, 234, 964
Spite, M., & Spite, F. 1991, A&A, 252, 689
Straniero, O., & Chieffi, A. 1991, ApJS, 76, 525 (Paper II)
Straniero, O., Chieffi, A., & Salaris, M. 1991a, in Proc. Workshop on Standard Candles (Trani), ed. F. Caputo (Mem. Soc. Astron. Italiana, Vol. 63), 315
———. 1991b, in Proc. Workshop on Star Clusters and Stellar Evolution (Teramo), ed. E. Brocato, F. Ferraro, & G. Piotto (Mem. Soc. Astron. Italiana, Vol. 63), 43
Tomkin, J., & Lambert, D. L. 1980, ApJ, 235, 925
Tomkin, J., Lambert, D. L., & Balachandran, S. 1985, ApJ, 290, 289
Tornambè, A. 1987, in Stellar Evolution and Dynamics in the Outer Halo of the Galaxy, ed. M. Azzopardi & F. Matteucci (Garching: ESO), 307
Van Altena, W. F., Lee, J. T., Hanson, R. B., & Lutz, T. E. 1988, in Calibration of Stellar Ages, ed. A. G. Davis Philip (Schenectady: Davis), 175
VandenBerg, D. A. 1985, in Production and Distribution of C, N, O Elements, ed. I. J. Danziger, F. Matteucci, & K. Kjar (Garching: ESO), 73
———. 1992, ApJ, 391, 685
VandenBerg, D. A., & Bell, R. A. 1985, ApJS, 58, 561 (VB85)
VandenBerg, D. A., & Stetson, P. B. 1991, AJ, 102, 1043
Zhao, G., & Magain, P. 1990, A&A, 238, 242
Zinn, R., & West, M. J. 1984, ApJS, 55, 45 (ZW84)